PREPARATION OF MOLYBDENUM-BASED CATALYSTS SUPPORTED ON ALUMINA FOR HYDRODESULFURIZATION OF LIQUID FUELS

BY

SADDAM AHMED GHALEB AL-HAMMADI

A Thesis Presented to the
DEANSHIP OF GRADUATE STUDIES

KING FAHD UNIVERSITY OF PETROLEUM & MINERALS

DHAHRAN, SAUDI ARABIA

In Partial Fulfillment of the
Requirements for the Degree of

MASTER OF SCIENCE

In

CHEMICAL ENGINEERING

April 2018

KING FAHD UNIVERSITY OF PETROLEUM & MINERALS

DHAHRAN- 31261, SAUDI ARABIA

DEANSHIP OF GRADUATE STUDIES

This thesis, written by **SADDAM AHMED GHALEB AL-HAMMADI** under the direction of his thesis advisor and approved by his thesis committee, has been presented and accepted by the Dean of Graduate Studies, in partial fulfillment of the requirements for the degree of **MASTER OF SCIENCE IN CHEMICAL ENGINEERING.**

A. Al Amer

Dr. Adnan M. Al-Amer
(Advisor)

Dr. Mohammed Ba-Shammakh
Department Chairman

Dr. Tawfik A. Saleh
(Member)

Dr. Salam A. Zummo
Dean of Graduate Studies

عمادة الدراسات العليا
DEANSHIP OF GRADUATE STUDIES

Shaikh Abdur Razzak

Dr. Shaikh Abdur Razzak
(Member)

18/4/2018

Date

To my Family

ACKNOWLEDGMENTS

All my appreciation and thanks to my thesis advisor, Prof. Adnan Al-Amer for his guidance and help all the way to the achievement of this thesis. He taught me Engineering Economics and Design Principles CHE 425 and encourage me to expand my knowledge in Chemical Engineering process designs. Many Thanks for his constant motivation and encouraging during my undergraduate and graduate studies.

I would like also to express my profound gratitude and deep regards to my committee member Dr. Tawfik Saleh for his constant encouragement, exemplary guidance and monitoring throughout my thesis research work. I can't thank him enough for hosting me in his Lab and allowing me to utilize his materials and equipment to achieve the objectives of my thesis project. I have shared with him lots of memorable memories inside and outside the lab and I considered him as a big brother. The encourage, guidance and help provided by him time to time will carry me a long way in my future life on which I am about to embark.

I would like also to thank my thesis committee member, Dr. Shaikh Abdur Razzak for his cooperation and constructive advice. Also, I would like to thank him for allowing me to work on one of his research projects which is related to fluidization technology and its modelling techniques during my bachelor's degree as a part of the Summer Training Course.

My deepest appreciation, thanks and acknowledgment to King Fahd University of Petroleum and Minerals (KFUPM) and Chemical Engineering Department for their full support during my bachelor and master's degrees.

With a special mention to my friends Nasser, Galal, Zaid, Qais, Zead, Akram, Nadham, Anwar, Omar, Islam and Mohammed Ameen, it was fantastic to have the opportunity to live in such a supportive and encouraging environment.

Finally, my ultimate thanks and love for my father, mother, wife, brothers and sisters for their endless support and love.

TABLE OF CONTENTS

LIST OF TABLES

LIST OF FIGURES

LIST OF ABBREVIATIONS

TP	Thiophene
BT	Benzothiophenes
DBT	Dibenzothiophene
MBT	Methylbenzothiophenes
DMBT	Dimethylbenzothiophenes
HDS	Hydrodesulfurization
EDS	Extractive Desulfurization
ADS	Adsorptive Desulfurization
ODS	Oxidative Desulfurization
BDS	Biodesulfurization
RADS	Reactive Adsorptive Desulfurization
NRADS	Nonreactive Adsorptive Desulfurization
γ-Al_2O_3	Gamma-alumian

AlMoCo	Alumina Loaded with MoCo Nanometals
AlMoNi	Alumina Loaded with MoNi Nanometals
AlMoCoB	Alumina Loaded with MoCo and B Nanoparticles
G	Graphene
AlMo	Alumina Loaded with Mo Nanometals
GNi	Graphene Loaded with Ni Nanometals
AlMoGNi	Alumina Loaded with Mo Nanometals and Doped with Graphene Loaded with Ni Nanometals
CNF	Carbon Nanofiber
AlCNF	Alumina-Carbon Nanofiber Composite
AlCNFMoCo	Alumina-Carbon Nanofiber Composite Loaded with MoCo Metals
TPD	Temperature Programmed Analysis by Desorption
TPR	Temperature Programmed Analysis by Reduction
XRD	X-Ray Diffraction
SEM	Scanning Electron Microscope

EDX	Energy-Dispersive X-ray Spectroscopy
ICP-MS	Inductively Coupled Plasma-Mass Spectrometry
TGA	Thermogravimetric Analysis
FTIR	Fourier Transform Infra-Red
TCD	Thermal Conductivity Detector
GC-SCD	Gas Chromatography Sulfur Chemiluminescence Detector
GC–MS	Gas Chromatography-Mass Spectrometry
$\mathbf{S_{BET}}$	BET Surface Area (m^2/g)
$\mathbf{S_{Meso}}$	Mesopore Surface Area (m^2/g)
$\mathbf{S_{Micro}}$	Micropore Surface Area (m^2/g)
$\mathbf{V_{micro}}$	Micropore Volume (cm^3/g)
$\mathbf{V_{total}}$	Total Pore Volume (cm^3/g)
APD	Average Pore Diameter (nm)
HF	Hierarchical Factor

DDS	Hydrogenolysis Reaction Pathway
HYD	Hydrogenation Desulfurization Pathway
BP	Biphenyl
THDBT	Tetrahydrodibenzothiophene
HHDBT	Hexahydrodibenzothiophene
CHB	Cyclohexylbenzene
BiCh	Bicyclohexyl

ABSTRACT

Full Name : [SADDAM AHMED GHALEB AL-HAMMADI]

Thesis Title : [Preparation of Molybdenum-based Catalysts Supported on Alumina for Hydrodesulfurization of Liquid Fuels]

Major Field : [Chemical Engineering]

Date of Degree : [April 2018]

Currently, crude oil is the main source of energy and raw materials for different industries around the world. However, the sulfur compounds, that usually exist in the produced oil, gasoline, diesel and jet fuel in a significant amount, have a tremendous number of negative impacts, such as, environmental pollution, reducing the efficiency of the engine, causing a severe corrosion to reactors, pipes and other equipment, and poisoning the catalysts. As a result, many countries have enforced strict environmental regulations and constraints to reduce the contained sulfur to the minimal level. To accomplish this goal, hydrodesulfurization (HDS), which includes a reaction between a liquid fuel and H_2 gas over a chosen catalyst at a high temperature and pressure, is implemented widely in most of the refinery plants. Conventionally, Mo catalysts supported on γ-Al_2O_3 and promoted by either Ni or Co nanoparticles are the most used catalysts for HDS process. In the current work, two modifications have been proposed to enhance the catalytic activity of γ-Al_2O_3 supported Mo catalysts and these modifications are:

1. γ-Al_2O_3-supported Mo catalyst doped with Ni nanoparticles loaded on graphene (AlMoGNi) was synthesized, characterized and evaluated for HDS of dibenzothiophene (DBT) and compared with the conventional γ-Al_2O_3-supported MoNi catalyst (AlMoNi). The catalytic activity of the prepared materials was evaluated in a batch reactor at T= 300

°C, and 53 bar hydrogen partial pressure. The decalin solvent was used as a model fuel containing 600 (ppm-S). The AlMoGNi reduced the sulfur concentration in the liquid fuel down to (11ppm-S, 99% sulfur removal) compared to (95 ppm-S, 84.2% DBT catalytic conversion) using AlMoNi catalyst within 5h reaction time at the targeted operating conditions. The better catalytic activity of AlMoGNi was attributed to its textural properties, surface acidity and nanoparticles dispersion.

2. Alumina-CNF nanocomposite support for MoCo catalyst (AlCNFMoCo) was prepared, characterized and tested for hydrodesulfurization of dibenzothiophene in liquid fuels. The AlCNFMoCo catalysts were compared with the corresponding conventional alumina-supported catalysts (AlMoCo). The alumina-CNF composite was prepared by sol-gel method and then loaded with Mo and Co nanoparticles by the incipient wetness impregnation method. The different types of the catalysts were characterized by N_2-physisorption, temperature programmed analysis by reduction, X-ray diffraction, scanning electron microscope, energy-dispersive X-ray spectroscopy etc. The BET surface areas of AlMoCo and AlCNFMoCo were 166 and 200 (m^2/g), respectively. The catalysts were evaluated by HDS reaction in a batch reactor at the following operating conditions: temperature of 300 ^oC, 55 bar H_2 partial pressure and 0.5g of the prepared catalyst. The model fuel was prepared using decalin as a solvent with 550 ppm-S. 97% and 85.8% sulfur removal were obtained using AlCNFMoCo and AlMoCo catalysts, respectively, indicating that doping CNF into γ-Al_2O_3 support has boosted the catalytic activity to desulfurize liquid fuels.

ملخص الرسالة

الاسم الكامل: صدام أحمد غالب الحمادي

عنوان الرسالة: تصنيع محفزات الموليبدينوم الكيميائية المستندة على أكسيد الألومنيوم من أجل إزالة الكبريت من وقود المحركات عن طريق تفاعل الهدرجة

التخصص: هندسة كيميائية

تاريخ الدرجة العلمية: ابريل 2018

في الوقت الحاضر، يعتبر النفط الخام هو المصدر الرئيسي للطاقة والمواد الخام لمختلف الصناعات في جميع أنحاء العالم. ومع ذلك، فإن مركبات الكبريت، التي توجد عادة بكميات كبيرة في مشتقات النفط مثل وقود المحركات النفاثة ، لها الكثير من الآثار السلبية، منها التلوث البيئي، والحد من كفاءة المحركات، وتسمم المحفزات الكيميائية في مصافي النفط و التسبب في تآكل شديد للمفاعلات الكيميائية، وأنابيب المصانع وغيرها من المعدات. نتيجة لهذه الأسباب قامت الكثير من الدول بفرض أنظمة وقيود بيئية صارمة للحد من الكبريت في المشتقات النفطية للحد الأدنى.

من الوسائل الفعالة لتحقيق هذ الهدف، هو تفاعل الهدرجة (اختصاراً HDS من Hydrodesulfurization) الذي يتضمن تفاعل غاز الهيدروجين مع الوقود السائل في وجود المحفزات الكيميائية تحت درجة حرارة مرتفعة وضغط شديد. يعتبر محفز الموليبدينوم Mo المستندة على أكسيد الألومنيوم Al_2O_3 والمحسن بالكوبلت Co أو النيكل Ni من المحفزات التقليدية التي تستخدم على نطاق واسع في مصافي البترول. في هذة الرسالة البحثية تم اقتراح ودراسة بعض التعديلات على هذة المحفزات التقليدية لجعلها أكثر فاعلية في عملية استخلاص الكبريت من الوقود السائل وهذة التعديلات كالتالي:

1. تم دمج مادة الجرافين المطعمة بجزئيات النانو لمعدن النيكل Ni مع أكسيد الألومنيوم المحمل بجزئيات النانو لمعدن الموليبدينوم Mo لتكوين المحفز الكيميائي الجديد الذي رمز له اختصارا ب AlMoGNi. هذا المحفز تم تصنيعه وتوصيفه وتقييم ادائه كمحفز كيميائي لتفاعل الهدرجة HDS لمركب ثنائي بنزو ثيوفينDBT وتم مقارنته بالمحفز التقليدي الذي رمز له اختصارا ب AlMoNi. تم تقييم النشاط التحفيزي للمواد

المحضرة في مفاعل عند درجة حرارة 300 درجة مئوية، و 53 بار ضغط جزئي هيدروجيني وتم استخدام مذيب ديكالين Decalin كوقود نموذجي يحتوي على 600 جزء في المليون من الكبريت (ppm-S). أثبت المحفز الكيميائي الجديد قدراته على استخلاص الكبريت بنسبة تصل الى 99% مقارنة مع نسبة قدرها 84.2% للمحفز التقليدي AlMoNi خلال فترة 5 ساعات من الوصول لظروف التفاعل المستهدفة. ويعزى النشاط التحفيزي الأفضل للمحفز الجديد إلى خصائصه التركيبية وحموضة السطح وتوزيع جسيمات النانو بشكل منتظم كما تم برهنت ذلك من خلال تجارب توصيف المحفزات الكيميائية.

2. تم دمج مادة ألياف الكربون النانونية CNF مع أكسيد الألومنيوم وتحميله جسيمات نانونية من معادن الموليبدينوم Mo والكوبلت Co لتكوين المحفز الكيميائي الجديد الذي رمز له اختصارا ب AlCNFMoCo وتمت مقارنته مع المحفز التقليدي المقابل له AlMoCo. تم تقييم النشاط التحفيزي للمواد المحضرة في مفاعل عند درجة حرارة 300 درجة مئوية، و 55 بار ضغط جزئي هيدروجيني وتم استخدام مذيب ديكالين Decalin كوقود نموذجي يحتوي على 550 جزء في المليون (ppm-S). أستطاع المحفز الكيميائي الجديد استخلاص الكبريت بنسبة تصل الى 97% مقارنة مع نسبة قدرها 85.6% للمحفز التقليدي AlMoCo خلال فترة 6 ساعات من الوصول لظروف التفاعل المستهدفة. وهذا يدل على فاعلية ألياف الكربون النانونية في زيادة النشاط التحفيزي لتفاعل الهدرجة من خلال زيادة مساحة السطح للمحفز وزيادة حموضة السطح وتحسين توزيع جسيمات النانو على المحفز الكيميائي.

CHAPTER 1

INTRODUCTION

Crude oil is a valuable source of energy and raw materials for most of the modern world industries. However, the existence of sulfur compounds such as dibenzothiophene (DBT), and dimethylbenzothiophenes (DMBT) creates a huge challenge in its utilization for different purposes because these compounds lead to tremendous number of environmental problems and increased cost of refining products due to catalysts poisoning, corrosion of refining pipes and equipment[1–4].

Sulfur compounds usually can be found in most of the oil fractions such as gasoline, jet fuels and diesel as impurities. The combustion of fuel which contains these sulfur compounds leads to release of SO_X compounds into the surrounding environment, creating lots of problems such as the environmental pollution and spreading of dangerous diseases[5–7]. Thus, the demand for high-quality fuels coupled with emerging strict environmental regulations and constrains make creating different techniques and developing the available ones for sulfur removal an urgent and important issue[8–10]. For example, in the United State of America (USA), the allowable sulfur concentration for gasoline and highway diesel were reduced to 30 ppm-S and 15 ppm-S, respectively, according to Environmental Protection Agency (EPA) regulations[11].

In the current work, a series of Mo catalysts that will be used for hydrodesulfurization (HDS) of liquid model fuels. Desulfurization is an important issue in the refining process

of crude petroleum products because sulfur-containing compounds cause environmental pollution, poison catalysts, and corrode refining equipment. There are ongoing efforts to lower the levels of sulfur in all kinds of oils and one of the major areas that have continued to attract tremendous attention is the fabrication of materials that act more effectively as adsorbent/catalyst compared to the existing ones. In this work, different methods will be proposed for modifying Mo catalysts for HDS of liquid fuels. These methods are focused on doping specific materials such as graphene, and carbon nanofiber (CNF). These materials will be characterized by different instruments including N_2-physisorption, temperature programmed analysis by desorption and reduction (TPD, TPR), X-ray diffraction (XRD), scanning electron microscope (SEM), and energy-dispersive X-ray spectroscopy (EDX), etc. Subsequently, these catalysts will be evaluated for their HDS efficiency of dibenzothiophene (DBT) in liquid fuels using a batch reactor.

1.1 Objectives

This research work aims to formulate different composite materials that can be used as an effective support for Mo catalyst in HDS application. The specific objectives are:

1. To develop two novel materials that can be used as effective catalysts for HDS reaction as follows:

a. A novel alumina-supported Mo catalyst doped with Ni nanoparticles loaded on graphene.

b. A novel alumina-CNF nanocomposite as a support for MoCo catalyst.

2. To Characterize the prepared catalysts using different techniques including: N_2-physisorption, temperature programmed analysis by desorption and reduction (TPD & TPR), X-ray diffraction (XRD), scanning electron microscope (SEM), energy-

dispersive X-ray spectroscopy (EDX), inductively coupled plasma (ICP-MS) and Fourier transform Infra-red (FT-IR).

3. To evaluate the performance of the prepared materials to the desulfurization of sulfur compounds in a batch reactor system.

4. To analysis the products sample using GC-MS and proposing different reaction mechanisms.

5. To propose different interpretations that explain the reaction and characterization results.

1.2 Significance

Although HDS has been adopted as a viable technique for the effective removal of sulfur from liquid fuels, the development of an ideal catalyst with an excellent activity continued to remain a challenge to researchers.

In this work, different modifications on the Mo-based catalysts will be investigated for HDS process. Although several studies have been conducted on the utilization of composite materials for HDS process, there are no reports on such modifications for HDS catalysts. Due to the nature of the prepared composite material, the prepared materials are expected to have a large surface area, well developed internal pore structure, and a higher degree of active sites dispersion. Thus, the prepared catalysts will show a higher performance compared to the available or reported catalysts. In addition, the use of these catalysts can be extended to other applications such as cracking process and fuel cell applications.

CHAPTER 2

LITERATURE REVIEW

The adverse effects of sulfur dioxide emission into the atmosphere on human health necessitate the enforcement of stringent environmental regulations on the allowable sulfur contents of transportation fuel. The prevailing environmental regulations stipulate low sulfur content in transportation fuels and this is attainable via catalytic processes that transform the sulfur-containing compounds in the fuel into hydrogen sulfide gas (H_2S) which can be easily separated from the liquid phase. Hydrodesulfurization (HDS) process is relevant to compliance with the environmental regulations as it is one of the effective methods for achieving nearly complete removal of organosulfur compounds from transportation fuels [11]. However, its ultimate efficiency requires significant improvements as the nature of some bulky organosulfur compounds entails continuous efforts in designing new and efficient catalytic materials. Moreover, the resistivity against H_2S by catalytic materials enables the removal of H_2S and thus is necessary for deep HDS of the refractory sulfur compounds [12].

2.1 Desulfurization Techniques

Many investigations have been focused on developing different other methods for sulfur removal from oil fractions, including hydrodesulfurization (HDS)[13–15], Extractive desulfurization (EDS) [16,17], adsorptive desulfurization (ADS) [18,19]oxidative

desulfurization (ODS) [20,21] and Biodesulfurization (BDS) [22–24]. Figure 1 showed the desulfurization methods based on its working mechanism and Table 1 exhibited many investigations that utilized the desulfurization techniques for sulfur removal at optimized operating conditions.

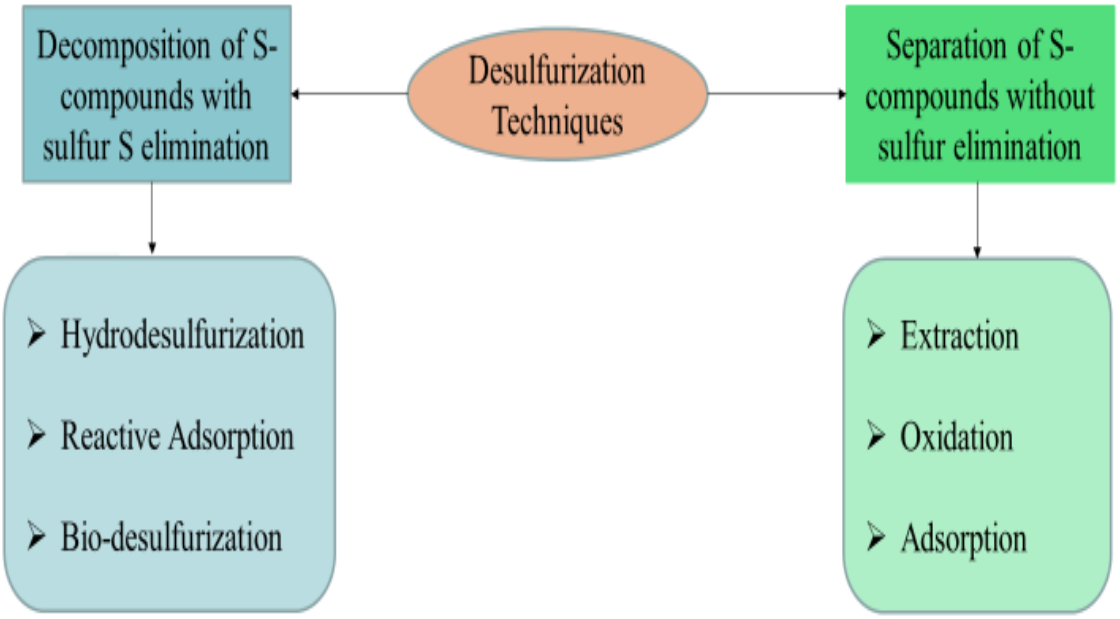

Figure 1 Classifications of desulfurization methods based on its working mechanism

HDS is the most common process that is used widely in refineries around the world, due to its high efficiency in removing sulfur with a high concentration from liquid fuels. The HDS includes the use of heterogonous catalysts at a relatively high temperature (250-500 °C) and at high hydrogen partial pressure (30-55 bar) to produce hydrocarbon fuel with less sulfur contents [25,26]. The common sulfur compounds, that are usually presented in oil fractions, are Thiophene (TP), benzothiophenes (BT), dibenzothiophene (DBT), methylbenzothiophenes (MBT) and dimethylbenzothiophenes (DMBT) [27]. These

compounds are stable aromatic contaminants, so they are difficult to remove from liquid fuels by the conventional methods such as adsorption process [28].

Extractive desulfurization (EDS) includes mixing the liquid fuel and certain solvents such as ethanol, acetone, and ionic liquids and followed by separation process to extract the targeted organosulfur compounds [29]. EDS is conducted without the need for catalysts or H_2 supply at ambient conditions. However, the main drawback of EDS process is the low solvent selectivity of certain sulfur compounds [30,31]. For example, acetone has low selectivity to compounds like thiophene and dibenzothiophene.

Adsorptive desulfurization (ADS) has two different types, namely, reactive adsorptive desulfurization (RADS) and nonreactive adsorptive desulfurization (NRADS). In RADS, suitable adsorbents are used at high temperature for sulfur removal while the remaining hydrocarbon compounds are recovered. The used adsorbents can be regenerated for reuse in other RADS process[32,33] . In the NRDS, the adsorption process can be done at room temperature and includes removal of sulfur compounds by physisorption on the surface of the used adsorbent [34,35].

Oxidative desulfurization (ODS) involves the oxidation of sulfur compounds by oxidants like hydrogen peroxide, acids, ozone and oxygen. Then, the extraction process is applied to separate the obtained sulfoxide or sulfones using a suitable solvent. The sulfones have higher polarity and can be removed easily by extraction process compared to benzothiophenes (BT) and related compounds. The suitable oxidant and a catalyst are utilized for the chemical conversion in the ODS [36,37].

Biodesulfurization (BDS) includes the utilization of microorganisms which have the inherent ability to transform/use the sulfur compounds thorough mainly metabolism process. BDS can be conducted at ambient operating conditions and it requires a microbial system with the capability to work on a wide range of sulfur compounds that usually can be found in oil fractions [38]. The advantage of BDS is the high selectivity towards sulfur compounds and the low waste production. On the other side, it is a slow process and obtaining biocatalysts with high efficiency is a challenging task [39].

Table 1 Sulfur removal by different desulfurization methods

Process	Materials/ Reagent/ Microorganism	Reactor Type	Sulfur Conc. ppm-S	Sulfur Removal %	T (^{o}C)	Refer
HDS	$CoMo/TiO_2$	Batch reactor	300	60.5%	300	[40]
	$NiMo/Al_2O_3$	Packed bed reactor	740	90%	350	[41]
	CoMo/SBA-15	Batch reactor	2160	77%	300	[42]
	$FeMoS/Al_2O_3$	Batch reactor	1000	30%	280	[43]
	Co-Mo-Al	Trickle bed	1800	20%	360	[44]
	Mo	Batch	350	99.5%	340	[45]
ODS	H_2O_2+formic acid	Batch	500	80%	50	[46]
	Na_2WO_4 /30% H_2O_2 /CH_3CO_2H	Batch	500	100%	70	[47]
	t-BuOOH / HPWA-SBA-15	Batch	174	97.43%	70	[48]
	K_2FeO_4	Batch	457	98%	35	[49]

	CeO_2/C based anode	Electrolysis Cell	310	83%	25	[50]
	H_2O_2 + Mo/Al_2O_3	Batch	320	97%	60	[51]
	H_2O_2/V_2O_5	Batch	500	99%	60	[52]
	H_2O_2/ Amphiphilic Catalysts	Batch	500	98%	40	[37]
ADS	Activated Carbon	Batch	178	95%	25	[53]
	Alumina	Packed Column	700	30%	200	[54]
	$NiMoP/Al_2O_3$ /NaY zeolite	Fixed Bed	450	56%	340	[55]
	Activated Carbon	Packed Column	300	88%	70	[56]
	Gallium + Y zeolite	Fixed Bed	500	97%	60	[57]
	Zeolites from coal fly ash	Batch	500	63	30	[58]
	CuCl/ $PdCl_2$ MCM-41/ SBA-15	Fixed Bed	841	94%	350	[59]
	MoCo/AC	Batch	300	95%	25	[19]
	MnO/AC	Batch	53	85%	25	[60]
	Mycobacterium goodii X7B	Fed Batch	200	99%	40	[61]
	Rhodococcus erythropolis IGTS8	Batch	200	80%	30	[62]

BDS	Bacterium, strain RIPI-22	Batch	100	77%	30	[63]
	Sphingomonas subarctica T7b	Fermentor	280	94%	27	[64]
	Microbacterium strain ZD-M2	Batch	36	94%	30	[65]
	Caldariomyces fumago	Batch	1600	99%	25	[66]
	Gordonia alkanivorans strain 1B	Batch	100	63%	35	[67]
	Rhodococcus erythropolis	Interface Bioreactor	184	90%	30	[68]
	Pseudomonas delafieldii R-8	Fermentor	591	47%	30	[69]

2.2 HDS Catalysts

The catalysts consist of two main components which are the active sites and the support. In the following sections, different active metals and support materials that are commonly used as HDS catalysts components are discussed.

2.2.1 Active Metals

Thus, HDS requires the use of catalysts with high efficiency and stability to ensure the sulfur removal to the required levels. MoS_2 catalysts supported on γ-Al_2O_3 is the most used catalysts that applied in HDS processes [11]. The catalysts are usually promoted with nanometals, such as, Ni and Co [70,71]. Furthermore, other types of catalysts have been improved and used for HDS, including transition metals phosphides such Ni_2P and Rh_2P [72,73]. Also, Ir, Pt [74], Au and Pd [75] can be used as catalysts for HDS processes.

Though lots of active catalysts have been used, developing catalysts with larger surface area, controlled pore size and volume, optimal dispersion of the active metals, and suitable acidity have remained a challenge and needs lots of effort, time and money to be achieved.

2.2.2 Catalysts Support

The active metals are supported on a specific material that works as a catalysts carrier. The support has certain requirements, including high surface area, good acidity, controlled pore size, and strong thermal and mechanical properties. The support of catalysts plays crucial role in the catalytic performance and stability of the prepared materials. Many kinds of materials have been utilized as a support for HDS catalysts, such as, Al_2O_3 [76], TiO_2 [77] , SiO_2 [78,79], ZrO_2 [80], zeolite [81] and carbonic materials [82,83]. However, γ-Al_2O_3 support is the most used support for HDS catalysts due to its strong mechanical characteristics and good acidic properties [12]. Some studies have investigated the combination of different types of supports to generate a support with unique characteristics in terms of surface area, pore size and volume and surface acidity. Examples of such combinations are TiO_2- Al_2O_3 [84], ZrO_2-Al_2O_3 , Al_2O_3-SiO_2 [85] and carbon- Al_2O_3 [86], and all of these supports showed better surface characteristics and acidic nature than the single support.

The metals-support interaction, and support nature acidity play important role in HDS catalyst performance. The interaction between the active species and the support affect significantly the metals dispersion and morphology of the active sites, which in turn, decrease/increase the catalytic activity of the prepared catalysts[11]. Strong interaction between the active metals and the support leads to low metals dispersion and makes their reducibility and sulfidability more difficult. Many investigations showed that strong

metals-support interaction leads to less Mo and Co metals dispersion and incomplete sulfidation process with remaining of Mo-O-Al linkages[87].

Furthermore, the acidity of the catalysts influences the catalytic performance the used materials. For example, SiO_2-Al_2O_3 composite support has strong acidic sites and it showed high catalytic HDS activity[88]. However, strong acidity is not enough for the catalysts to approve as an effective catalyst for HDS process. For example, zeolite has a strong acidity, especially Bronsted acidic sites that boost the catalytic activity of the zeolite support. However, zeolite has not been the first choice the HDS support catalysts, since it is more difficult for the active metals to be impregnated and dispersed on its highly crystallin structure. The zeolite pore size is too small for metals, such as, Mo, Co and Ni to be accommodated and also for sulfur compound to be adsorbed [89]. Figure 2 showed different important factors for developing catalysts with high stability and activity.

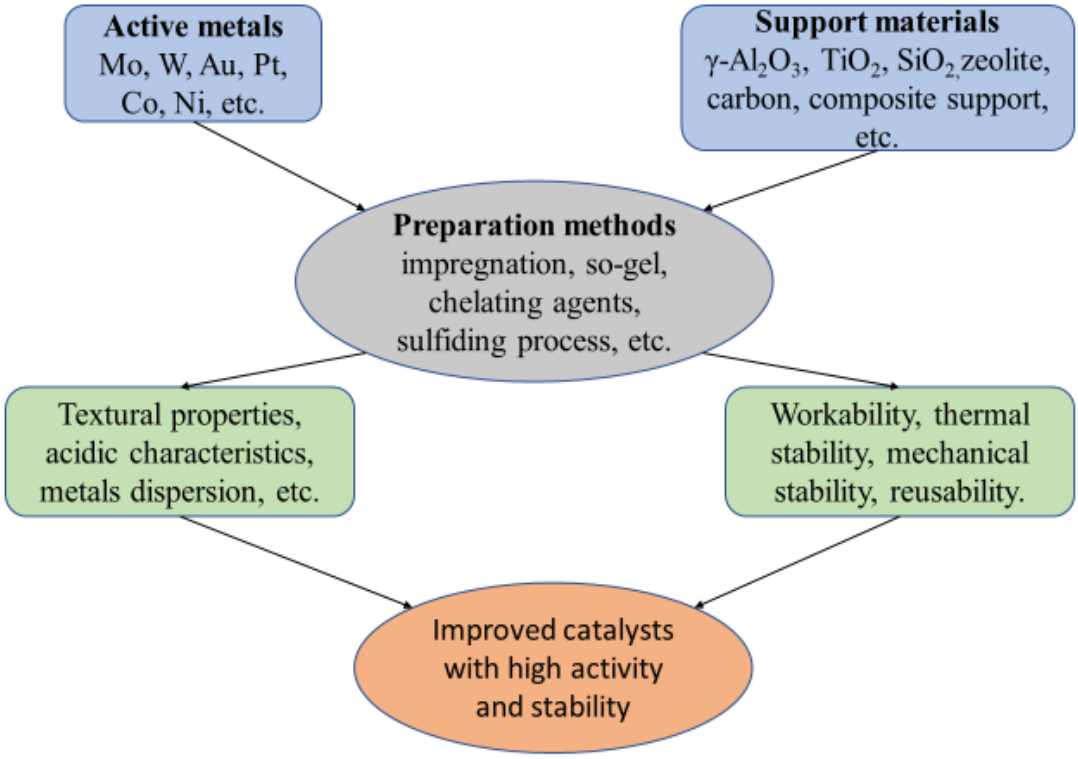

Figure 2 Factors that influence the synthesis of improved catalysts

2.2.3 Effect of Additives

The HDS catalysts can be improved by adding some additives to the support such as B, F, Na, Zn and P. It has found that these additives modified the acidic and basic characteristics of the support, which in turn, influence the metals-support interaction, metals dispersion and ultimately the HDS catalytic activity [90].

Recently, the most used additive is P that is well-reported for enhancing the HDS catalytic activity. Other researchers focused on Na and they reported that Na boost the reducibility and sulfudibility of the active species. Also, B is used to control the acidity of the catalysts and to improve its catalytic activity [91].

CHAPTER 3

METHODOLOGY

In this chapter, different catalysts synthesis methods have been described. Also, materials characterization and catalytic evaluation techniques have been discussed.

3.1 Materials Preparation

3.1.1 Synthesis of Graphene

The graphene was prepared from graphite by using modified Hummers'method. About 10 g of graphite and 3 g of sodium nitrate were added into 500 mL sulfuric acid into a 3 L beaker equipped with a teflon impeller. Then, the mixture was stirred at zero oC. After that, about 30 g of potassium permanganate ($KMnO_4$) was slowly introduced into the mixture. The mixture was stirred continuously at room temperature. After that, 500 mL of water was added. In order to reduce residual permanganate to soluble manganese ions, 30 % hydrogen peroxide (H_2O_2) was slowly added and vigorous bubbles appeared as the color of the suspension changed from dark brown to yellow. The suspension was centrifuged at 10,000 rpm to obtain the graphene oxide.

3.1.2 Synthesis of AlMoNi and AlMoGNi Catalysts

There are two types of the prepared catalysts: (1) Mo catalyst support on γ-Al_2O_3 and promoted by Ni nanoparticles (AlMoNi) (2) Mo catalysts supported on γ-Al_2O_3 and promoted by Ni nanoparticles supported on graphene (AlMoGNi).

The commercial alumina was heated up to 500 °C to obtain γ-Al_2O_3. Then, the γ-Al_2O_3 support was loaded with 15 wt% Mo nanometals by incipient wetness impregnation method. 6.4 g of γ-Al_2O_3 was added to 100 ml of deionized water with stirring at 70 °C for 15 minutes. Then, 100 ml of aqueous solution of 2.23 g ammonium molybdate $(NH_4)_6Mo_7O_{24}.4H_2O$ was added to the dispersed alumina and kept with stirring at T=80 °C for 6h.

To prepare the first type of the catalyst, 100 ml of aqueous solution of 1.7g nickel acetate $Ni(OCOCH_3)_2.4H_2O$ was added to the mixture with stirring at T=80 °C for 5h. Then, the solid catalysts were separated from the aqueous solutions by HERMLE centrifuge and the resultant sample was dried at 100 °C for 5h. Finally, alumina-supported MoNi catalyst was calcined at 300 °C for 3h.

To prepare the second type of the catalyst, graphene was loaded with Ni nanoparticles using the sol-gel method. A small amount of graphene (0.01 wt%) was added to 100 ml of aqueous solution of nickel acetate $Ni(OCOCH_3)_2.4H_2O$ and the mixture was refluxed at 120 °C for 4h. The resultant sample was added to the prepared alumina-supported Mo catalyst and the mixture was refluxed at 120 °C for 5h. following the same conditions as the first type of the catalyst, the solid materials were separated, dried and calcinated. Figure 3 contains the steps for preparing AlMoGNi catalyst and supported with photos for more illustration.

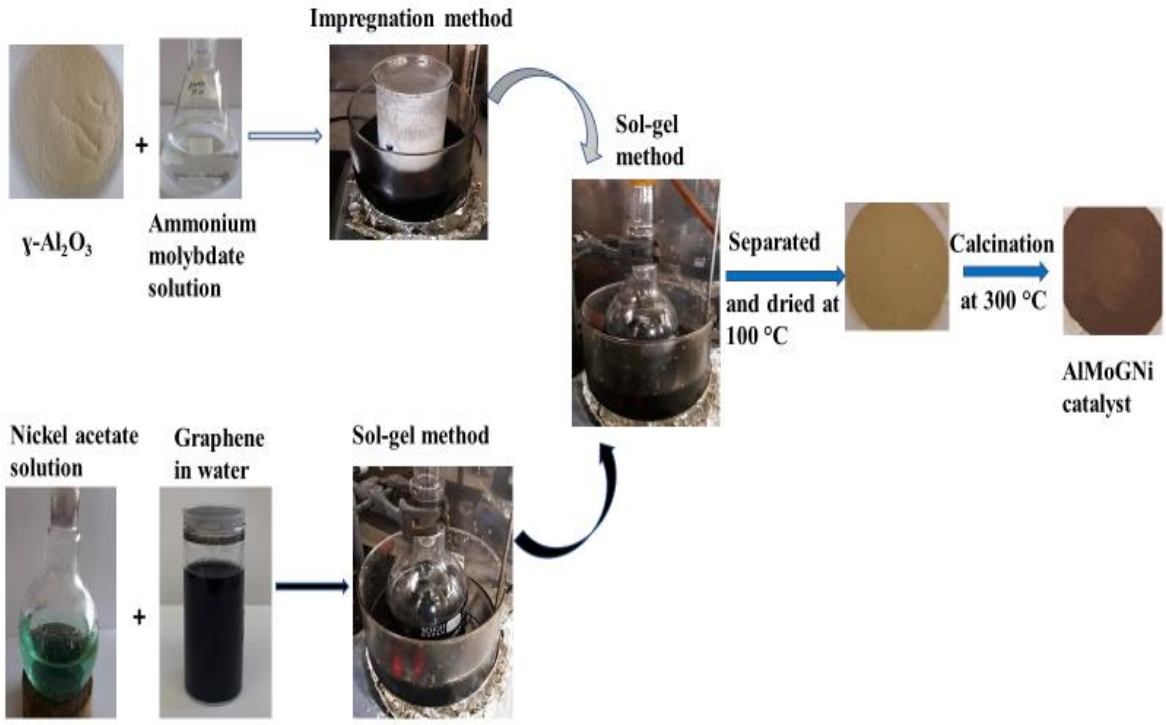

Figure 3 Preparing steps of AlMoGNi catalyst

3.1.3 Synthesis of AlMoCo and AlCNFMoCo Catalysts

The commercial alumina was heated to 500 °C to obtain gamma-alumina. Around 9.5 g of the gamma-alumina was mixed with 0.5 g of carbon nanofiber (CNF) to obtain carbon nanofiber-doped alumina using the sol-gel method. The mixture was mixed with 100 ml of deionized water, 10ml ethanol, and 5ml diethylene glycol and stirred for 1h. The mixture was refluxed at 110 °C for 6 h, and the precipitate was separated and dried at 100 °C.

The AlCNF composite was loaded with Mo and Co nanoparticles with percentages of 15% and 5%, respectively, using the incipient wetness impregnation method. 80 ml of deionized water was added to 4.8 g of the prepared AlCNF under stirring at 85 °C for 35 minutes. Then, 100 ml of aqueous solution containing 1.66 g of ammonium molybdate and 1.46 g

cobalt nitrate were added to the dispersed alumina and kept under stirring at T=85 °C for 3 h. During the stirring, 5 ml of diethylene glycol was added to enhance the connection between the nanoparticles and the alumina support. The resultant mixture was filtered and dried at 100 °C for 5h. The prepared catalyst was calcined at 350 °C. The preparation steps of the AlCNFMoCo were clearly shown in Figure 4 for better illustration. The same method was used to load gamma-alumina with MoCo metals, without doping with CNF, for comparison purposes.

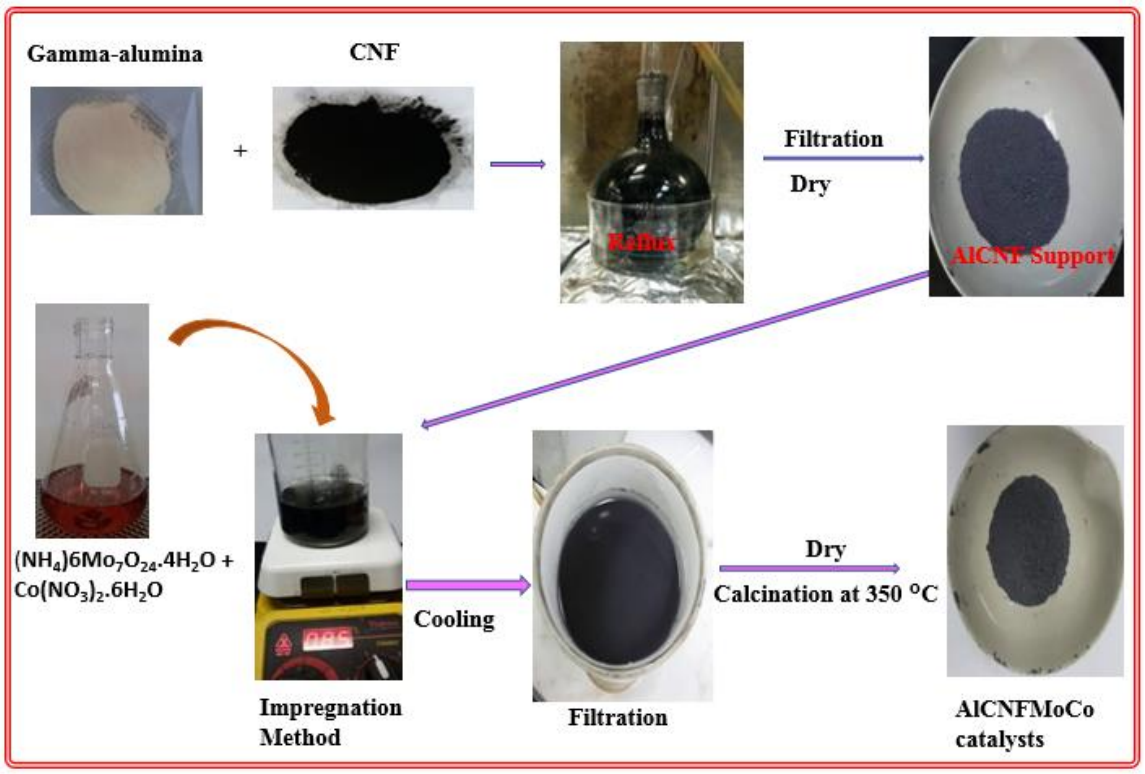

Figure 4 Illustration of the steps used in preparing AlCNFMoCo Catalysts

3.2 Catalysts Characterization

The prepared catalysts were characterized for their structural and morphological properties by N_2-physisorption, temperature programmed analysis by desorption and reduction (TPD and TPR), X-ray diffraction (XRD), scanning electron microscope (SEM), energy-

dispersive X-ray spectroscopy (EDX), inductively coupled plasma (ICP) and Fourier transform Infra-red (FTIR).

N_2 adsorption-desorption isotherms were obtained to determine the BET surface areas, pore volumes, and pore size distributions. Measurements were taken using a micromeritics TriStar II Plus automatic analyzer and with all samples degassed ($p < 10{-}1$ Pa) at 150 °C for 4h before the experiments.

The reducibility potential of metal oxides was determined by temperature-programmed reduction (TPR) with hydrogen as the probe molecule using a Micromeritics (AutochemII-2920) chemisorption analyzer. Approximately 40 mg of the catalysts were pre-treated for one hour in high-purity helium at 500 ˚C and then cooled to ambient temperature before being heated to 850 ˚C at 10 ˚C/min under a steady flow (20 ml/min) of 10% H_2 in helium. The consumption of H_2 at the reducible temperature(s) was recorded on a thermal conductivity detector (TCD).

Surface acidity was measured by temperature-programmed desorption of ammonia (NH_3-TPD) using a MicromeriticsChemisorb 2750 (pulse chemisorption system) with 10 wt.% NH_3. Approximately 70 mg of the catalyst was loaded into a quartz tube and covered with quartz. The sample was purged with high purity helium at 600 ˚C and held for 30 min before being cooled to 100 ˚C. The probe molecule (NH_3) was adsorbed on the sample at 100 ˚C for 30 min, which was followed by helium purging for 60 min to remove any physisorbed ammonia. NH_3 desorption was accomplished by heating the furnace at 10˚C/min to 900 ˚C, and the data were recorded with a thermal conductivity detector (TCD).

The X-ray diffraction pattern of the adsorbent was taken using (Rigaku Miniflex II desktop X-ray powder diffractometer) using Cu-K radiation and an X-ray gun operated at 40 kV (voltage), 200 mA current and λkα1 = 1.54Å using powdered samples. Data were collected from 2 = 10–80° at a scan rate of 2°/min and a step size of 0.02°.

Scanning Electron Microscope JEOL – JSM6610LV was used to examine the morphology of the studied adsorbent materials using secondary electron (SE) and back scattered electron (BSE) mode at an accelerating voltage of 20 kV, and the attached energy dispersive X-ray spectrometer (EDS, Oxford Inc.) detector was used for subsequent elemental analysis.

Fourier transform infrared spectroscopy (FT-IR) was used to identify the various functional groups present on the bare support and the catalysts supported by the carbon support using a Nicolet 6700 spectrometer (Thermo Electron). Pellets of the samples were made by adding KBr as a binder and then the absorption spectra obtained 64 scans.

3.3 Catalytic Evaluation

The HDS activity of the catalysts was evaluated using a batch reactor, model 4848B, which was purchased from the Parr Instrument Company. The HDS system is composed of a reactor, a hydrogen cylinder, gas controller, and the valves for controlling input and output samples, as shown in Figure 5. The HDS reaction occurred at T = 300 °C and (50-55) bar hydrogen partial pressure. About (0.5-0.6) g of the catalyst was inserted in the reactor vessel with 100 ml of a decalin solvent as a model fuel containing DBT at an initial concentration of 500-650 ppm-S. Each test was carried out for (5-6) h after achieving the target process conditions. When the temperature of the reaction was increased up to 300

°C, the first sample was collected by a manual valve and considered as a zero-hour sample. Then, samples were collected five times in the next 5/6 hours. The sulfur content in the feed was quantified using a gas chromatography sulfur chemiluminescence detector (GC-SCD). The products were identified by a gas chromatography-mass spectrometry (GC–MS). All the prepared catalysts samples were tested for the HDS reaction.

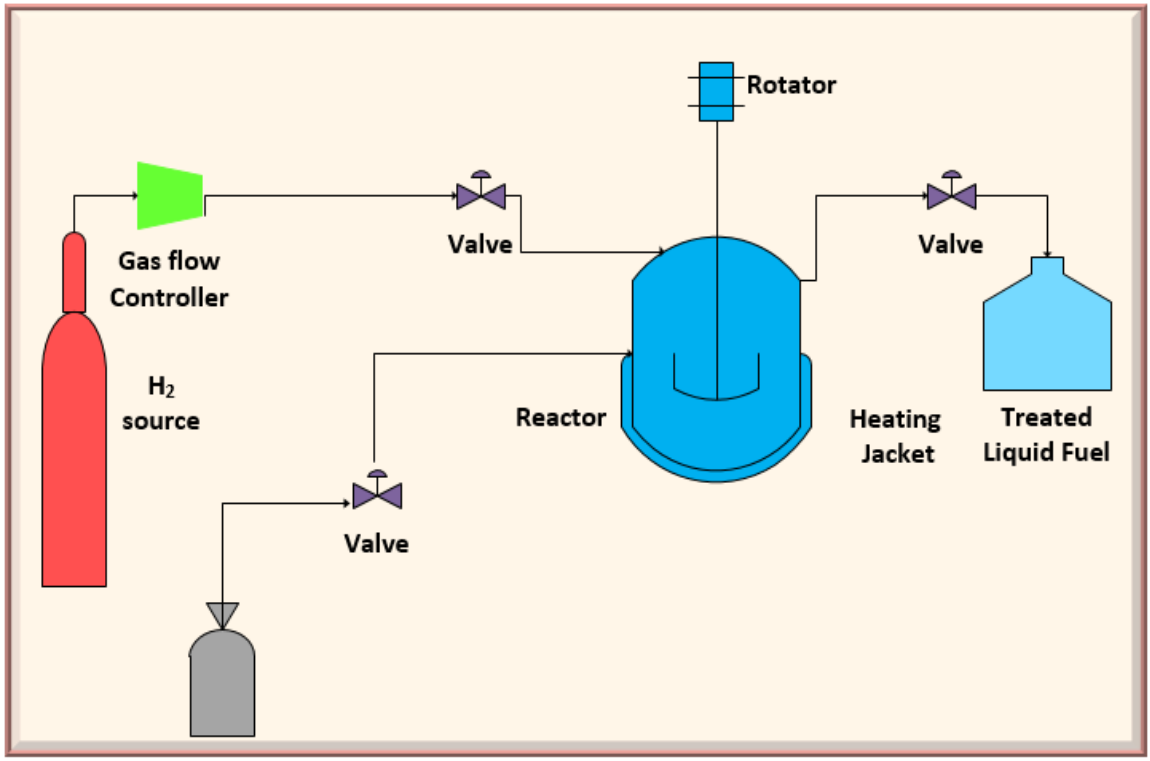

Figure 5 Schematic diagram of the used system for HDS reaction

CHAPTER 4

A Novel Alumina-supported Molybdenum Catalyst Doped with Nickel Nanoparticles Loaded on Graphene

Abstract

Alumina-supported Mo catalyst doped with Ni nanometals loaded on graphene (AlMoGNi) was synthesized, characterized and evaluated for hydrodesulfurization of dibenzothiophene and compared with the conventional alumina-supported MoNi catalyst (AlMoNi). The prepared catalysts were characterized by N_2-physisorption, temperature programmed analysis by desorption and reduction, X-ray diffraction, scanning electron microscope, energy-dispersive X-ray spectroscopy, inductively coupled plasma and Fourier transform Infra-red. The catalytic activity of the prepared materials was evaluated in a batch reactor at T= 300 °C, and 53 bar hydrogen partial pressure. The decalin solvent was used as a model fuel containing 600 parts per million sulfurs (ppm-S). The AlMoGNi reduced the sulfur concentration in the liquid fuel down to (11ppm-S, 99% sulfur removal) compared to (95 ppm-S, 84.2% sulfur removal) using AlMoNi catalyst. The better catalytic activity of AlMoGNi was attributed to its textural properties, surface acidity and nanoparticles dispersion. The reaction mechanism investigation revealed that the HDS over the prepared catalysts occurred through both hydrogenolysis and hydrogenation desulfurization pathways.

4.1 Introduction

Currently, crude oil is the main source of energy and raw materials for different industries around the world. However, the sulfur compounds, that usually exist in the produced oil, gasoline and jet fuel in a significant amount, have number of negative impacts, such as, environmental pollution, reducing the efficiency of the engine causing severe corrosion to the reactors, and poisoning the catalysts [92]. As a result, many countries have enforced strict environmental regulations and constrains to reduce the contained sulfur to minimal level [93–95].

To accomplish this goal, hydrodesulfurization (HDS), which includes a reaction between a liquid fuel and H_2 gas over a chosen catalyst at a high temperature and pressure, is implemented widely in most of the refinery plants [12]. The activity and stability of the chosen catalysts for HDS are playing a critical role in determining the efficiency of this process in removing the sulfur compounds from crude oil and its fractions [96]. Thus, producing more efficient catalysts and developing the available ones are urgent issues to ensure a high HDS performance with less energy consumption.

Traditionally, the MoS_2 catalysts supported on γ-Al_2O_3 and promoted by either Ni or Co are the most used catalysts for HDS process[97]. One of the important factors that influence the catalytic perforamcne of HDS is the chemical and textural properities of the used support. The support material is a main component of the catalyst structure and could increase or decrease its activity and stability. The common support of HDS catalysts are γ-Al_2O_3 [98–100] ,silica[78,85], carbon[101,102], zeolite[13,103,104], titania[105–107], zirconia[108,109], and SBA-15 [110,111]. Many invesigations are focused on improving

the chemical, mecnhanical and textural characteristics of the catalysts support to enhance its HDS activity using different methods [11].

Recently, many investigations have focused on carbon-modified supports to enhance the catalytic activity of the heterogenous catalysts using materials as a carbon source, such as, monocarboxylic acids[112], and citric acid [113]. Carbon-modified supports have attracted a great deal of scientific interest and showed promising results in improving the conventional supports of catalysts.

Graphene, which is a new form of carbonic materials, have excellent chemical, physical, thermal, electronic and mechanical characteristics with high specific surface area [114,115]. Thus, graphene-based materials have potential application in different areas, including, photocatalysis[116], catalysis[117,118] , sensing platforms[119] and energy storage[120]. Different studies used graphene-based as a support for HDS reaction [121–123]. Wang et al. (2015) [124] utilized graphene-modified TiO_2 support for NiMo catalysts to desulfurize liquid fuel containing dibenzothiophene (DBT). They found that the graphene-modified catalysts showed a higher HDS activity compared to corresponding unmodified catalysts.

To our best knowledge, there is no report on Mo catalyst supported on γ-Al_2O_3 (AlMo) and doped with graphene loaded with Ni nanoparticles (GNi). In the current study, we fabricated this catalyst and used it for HDS of DBT in the liquid fuel. The activity of the new catalyst (AlMoGNi) was compared with the corresponding conventional alumina-supported MoNi catalyst (AlMoNi). The prepared catalysts were characterized by N_2-physisorption, temperature programmed analysis by desorption and reduction (TPD /TPR),

X-ray diffraction (XRD), scanning electron microscope (SEM), energy-dispersive X-ray spectroscopy (EDX), inductively coupled plasma (ICP) and Fourier transform Infra-red (FTIR).

4.2 Catalytic Performance Evaluation

The HDS activity of the catalysts was evaluated using a batch reactor, model 4848B, which was purchased from the Parr Instrument Company. The HDS system is composed of a reactor, a hydrogen cylinder, gas controller, and the valves for controlling input and output samples, as shown in Figure 5. The HDS reaction occurred at T = 300 °C and 53 bar hydrogen partial pressure. About 0.6 g of the catalyst was inserted in the reactor vessel with 100 ml of a decalin solvent as a model fuel containing DBT at an initial concentration of 600 ppm-S in. Each test was carried out for 5 h after achieving the target process conditions. When the temperature of the reaction was increased up to 300 °C, the first sample was collected by a manual valve and considered as a zero-hour sample. Then, samples were collected five times in the next 5 hours. The sulfur content in the feed was quantified using a gas chromatography sulfur chemiluminescence detector (GC-SCD). The products were identified by a gas chromatography-mass spectrometry (GC–MS). Different HDS reactions were carried out with AlMoNi and AlMoGNi catalysts.

4.3 Results and Discussion

4.3.1 Surface and Textural Properties

In Figure 6a, N_2 adsorption/desorption isotherm curves of the prepared catalysts were displayed. The AlMoNi catalyst showed an isotherm of type IV, and also AlMoGNi catalyst has a typical isotherm of type IV. The micropores and mesopores were presented

in both catalysts, as indicated by nitrogen uptake at low relative pressure values and a hysteresis loop at high relative pressures, respectively.

The textural properties of AlMoNi and AlMoGNi catalysts were summarized in Table 2, including BET surface area, mesopore surface area, micropore surface area, micropore volume, total pore volume, average pore diameter and hierarchical factor (HF). It can be noticed that doping GNi to AlMo has enhanced both the surface area and pore volume of the catalyst compared to the conventional AlMoNi catalyst. For example, mesopore surface area of AlMoGNi, which is a very important factor for the efficiency of HDS reaction, was about 1.36 times that one in AlMoNi catalyst. However, AlMoNi and AlMoGNi have a close overall average pore diameter which were 7.4 and 7.3 nm, respectively, as shown in Figure 6b.

The HF was used to indicate the extent of the balance of the pore nature and volume of the prepared catalysts and was cacluated based on equation (1).

$$F = (V_{micro}/V_{total}) * (S_{meso}/S_{BET}) \qquad (1)$$

As shown in Table 2, the AlMoGNi catalyst has a higher HF value than the one of AlMoNi catalyst, indicating that AlMoGNi has a better adsorption efficiency [125], which in turn, increases its HDS catalytic activity.

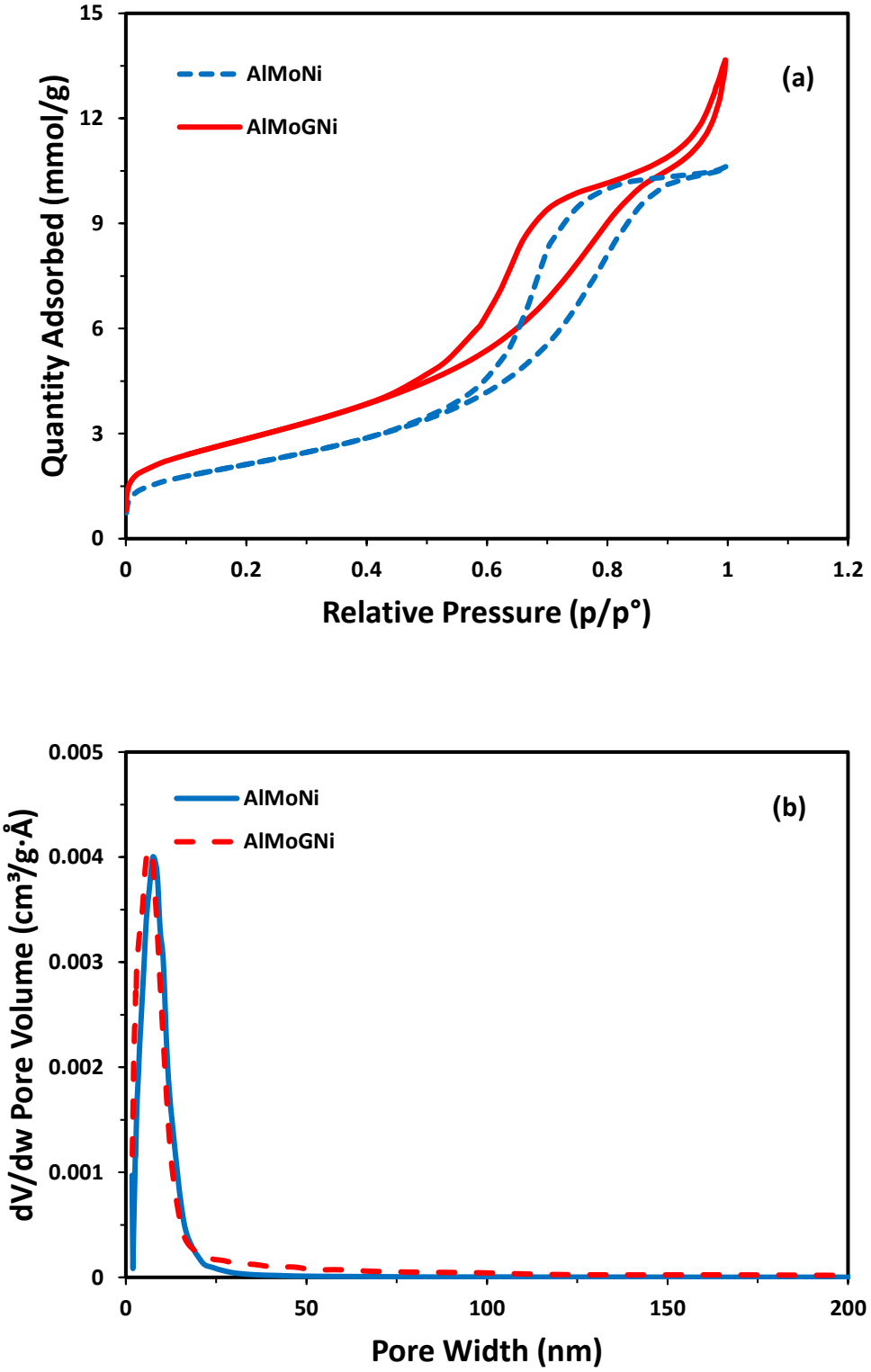

Figure 6 (a) N_2 adsorption/desorption isotherm (b) pore size distribution of the prepared catalysts

Table 2 Characterics of AlMoNi and AlMoGNi catalysts obtained from N_2 physisorption analysis.

Catalysts	S_{BET}[1]	S_{Meso}[2]	S_{Micro}[3]	V_{micro}[4]	V_{total}[5]	APD[6]	HF
AlMoNi	173.7	167.6	6.1	0.000249	0.3599	7.4	0.000667
AlMoGNi	234.2	227.2	6.8	0.000626	0.3894	7.3	0.001560

[1] m^2/g, [2] t-plot external (m^2/g), [3] t-plot micropore (m^2/g), [4] t-plot (cm^3/g), [5] total pore volumes (cm^3/g), [6] average pore diameter (nm).

4.3.2 XRD

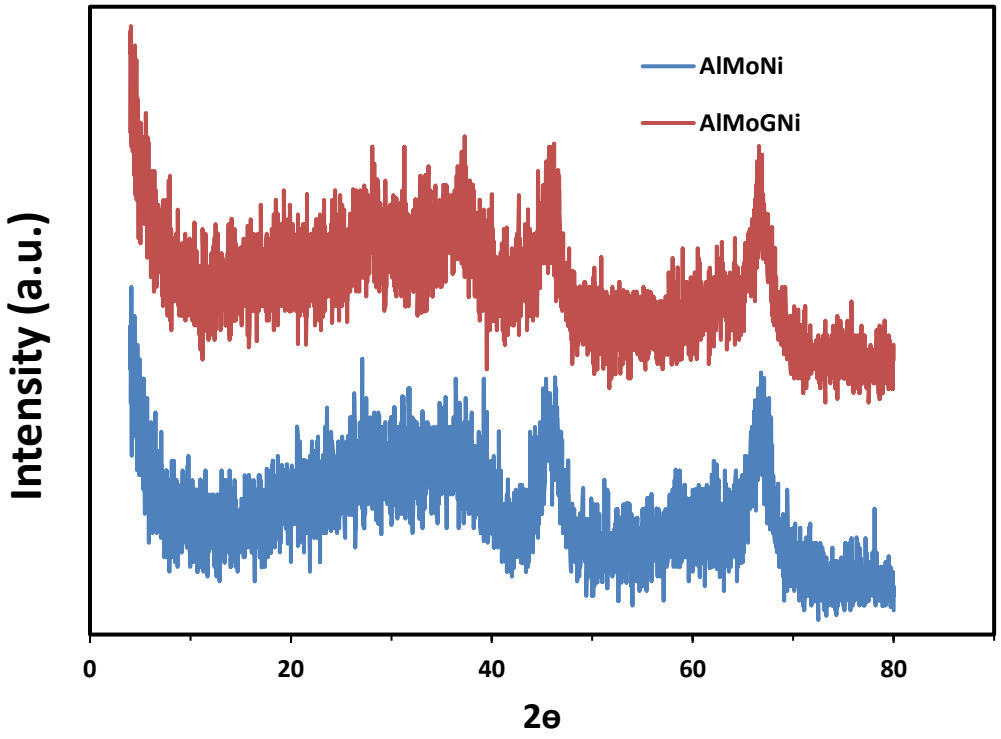

Figure 7 XRD results of AlMoNi and AlMoGNi catalysts

XRD patterns of the prepared catalysts showed in Figure 7. XRD results for both AlMoNi and AlMoGNi catalysts showed diffraction peaks at 2θ of 46° and 67° which are ascribed to γ-Al_2O_3. It can be observed that there are no peaks related to Mo and Ni phases which can be attributed to the high metals dispersion on the support [86,126]. Also, no diffraction peaks for graphene were observed in the AlMoGNi diffraction curve that is can be explained by the very small amount of the graphene in the catalyst, resulting in very low diffraction intensity of graphene [127,128]. Based on this, it can be concluded that the crystalline phase of γ-Al_2O_3 didn't change with GNi doping.

4.3.3 H_2-TPR

H_2-TPR was used to study the effect of doping GNi on the interaction of the MoNi nanoparticles and the catalyst support by characterizing the nanometals reduction on the γ-Al_2O_3 support. The H_2-TPR results of AlMoNi and AlMoGNi catalysts were exhibited in Figure 8. Both types of catalysts showed reduction peak at 350–420 ◦C, the temperature peak is usually assigned to the first step of reduction(Mo^{6+}-Mo^{4+}) of polymeric octahedral Mo species bonded to surface of the support weakly [129]. The higher temperature with a maximum 700–770 ◦C is ascribed to the second step of reduction(Mo^{4+}-Mo^{0}) of polymeric octahedral Mo and isolated tetrahedral Mo species interacted with the support strongly [130]

From Figure 8 and Table 3, it can be observed that the reduction temperatures of the active sites in AlMoGNi catalyst have a lower value than the corresponding ones in AlMoNi catalyst. This indicates that doping GNi reduced the metal-support interaction, resulting in a better dispersion of active sites on the surface of the catalysts. Thus, it expected that AlMoGNi will show a better catalytic performance compared to the counterpart catalysts.

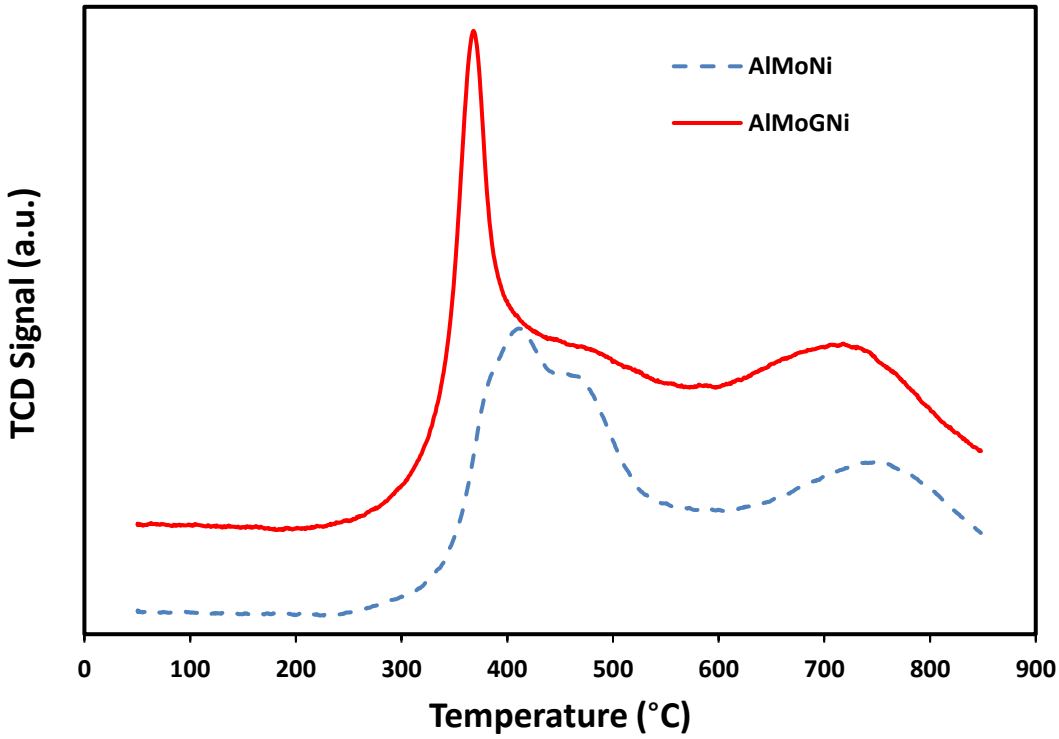

Figure 8 H_2-TPR results of AlMoNi and AlMoGNi catalysts

4.3.4 NH_3-TPD

NH_3-TPD is utilized to measure the acidic characteristics of the prepared catalysts. The NH_3-TPR results of AlMoNi and AlMoGNi catalysts were shown in Figure 9 and Table 3. The absorption of NH_3 usually classified as chemical and physical absorption. Both catalysts showed a chemical absorption of NH_3, since the NH_3 is desorbed at high temperatures between 150-780˚C.

Based on NH_3 desorption temperature, the acidic sites are categorized as strong (> 430 ˚C), medium (230-430 ˚C) and weak (<230 ˚C)[130].In both AlMoNi and AlMoGNi catalysts, the nature of the acidity was characterized as Lewis acid sites and they can classify as weak

and strong at temperature ranges of 150-230 ˚C and 450-780˚C, respectively. As shown in Figure 9 and Table 3, the NH_3-TPD results of AlMoGNi catalyst showed intensive desorption peaks and higher acidity compared to AlMoNi catalyst, indicating that doping GNi has enhanced the acidity of the AlMo catalyst.

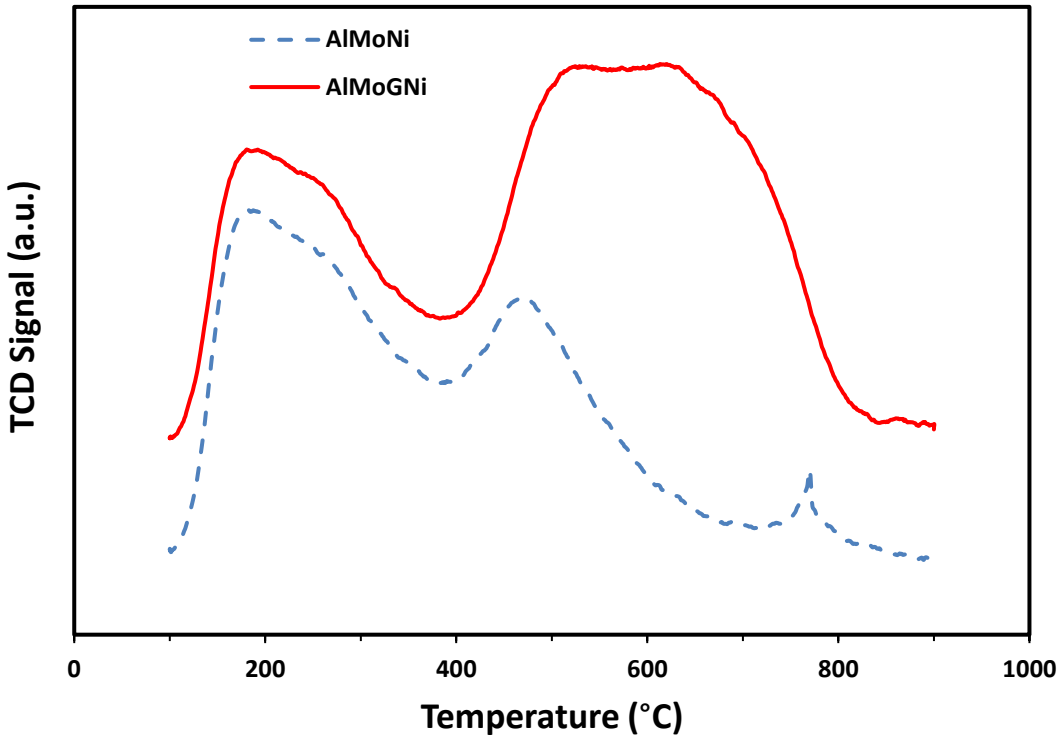

Figure 9 NH_3-TPD results of AlMoNi and AlMoGNi catalysts

Table 3 TPR and TPD measurement results of the prepared catalysts

Catalyst	H_2-TPR			NH_3-TPD		
	Temperature at Maximum (°C)	Quantity (mmol/g)	Total quantity (mmol/g)	Temperature at Maximum (°C)	Quantity (mmol/g)	Total acidity (mmol/g)

AlMoNi	409.63 750.21	1.614 0.225	1.839	177.95 470.02 769.46	0.231 0.036 0.004	0.271
AlMoGNi	367.87 718.08	1.599 0.3340	1.933	180.74 622.73	0.246 0.575	0.821

4.3.5 SEM/EDX and TEM

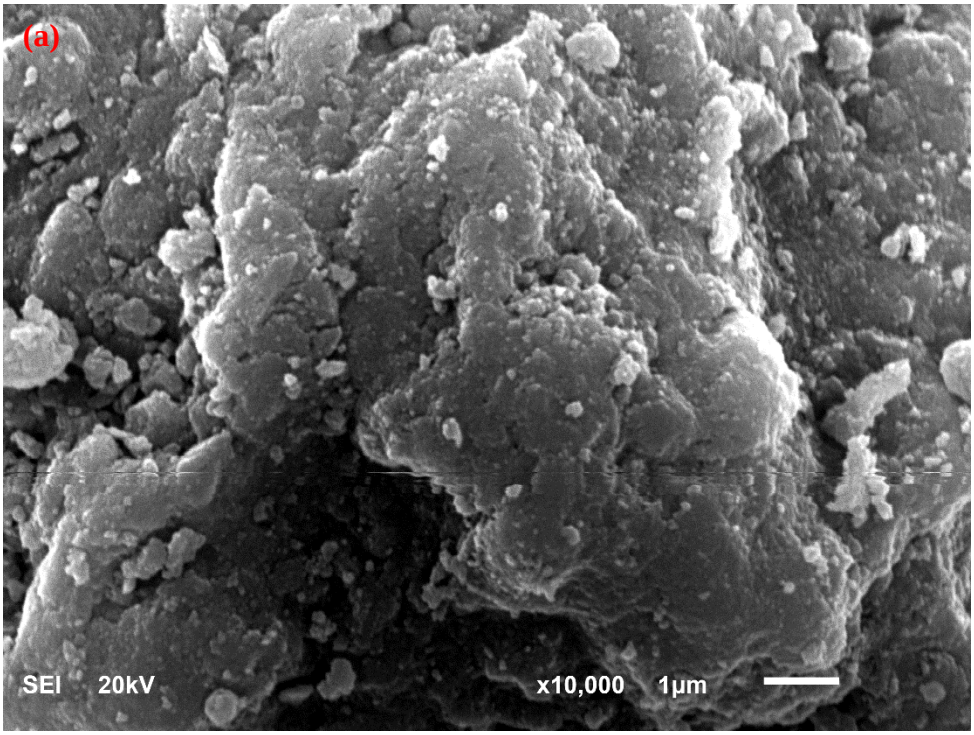

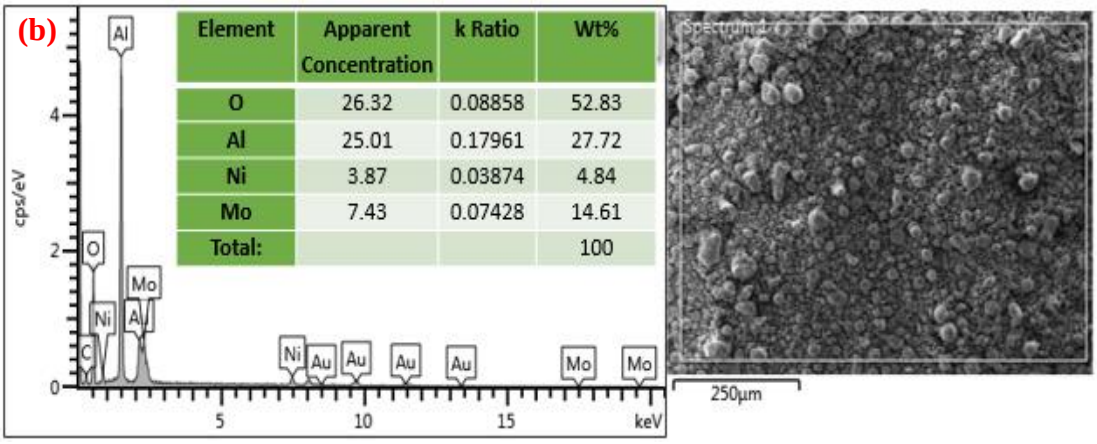
(b)
Element
Apparent Concentration
k Ratio
Wt%
O
26.32
0.08858
52.83
Al
25.01
0.17961
27.72
Ni
3.87
0.03874
4.84
Mo
7.43
0.07428
14.61
Total:
100
cps/eV
keV
250µm

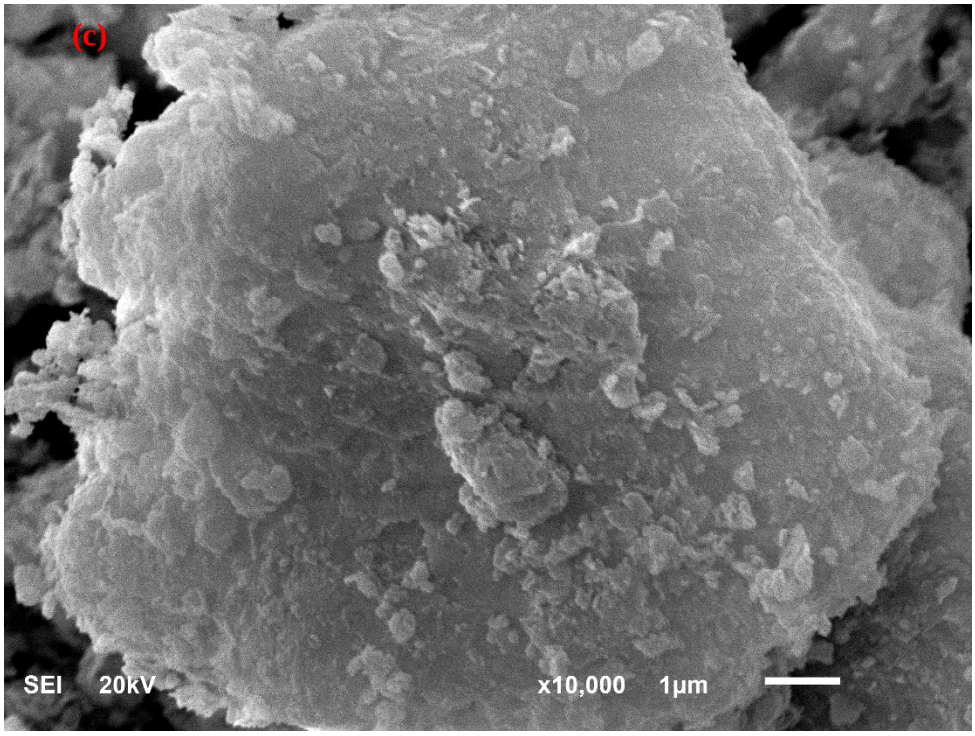
(c)
SEI 20kV
x10,000 1µm

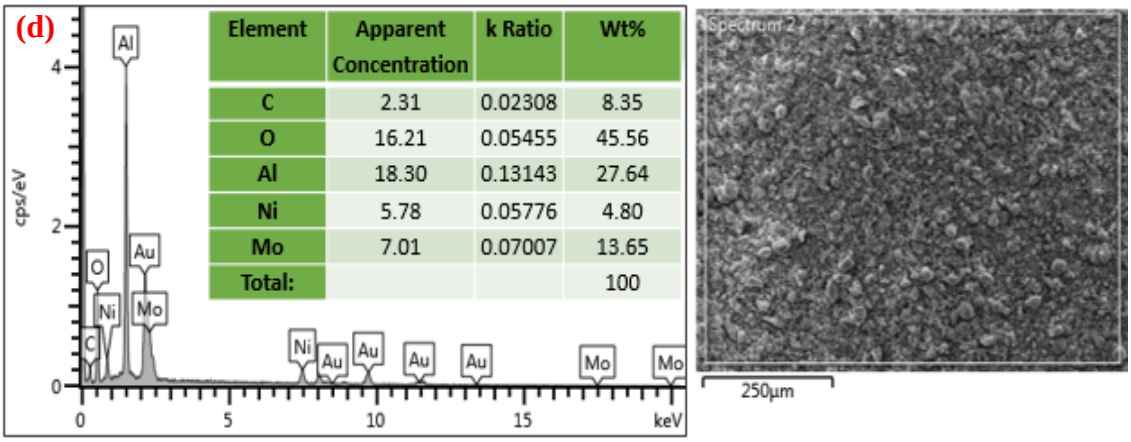

Figure 10 The SEM/EDX of (a) AlMoNi, and (b) AlMoGNi.

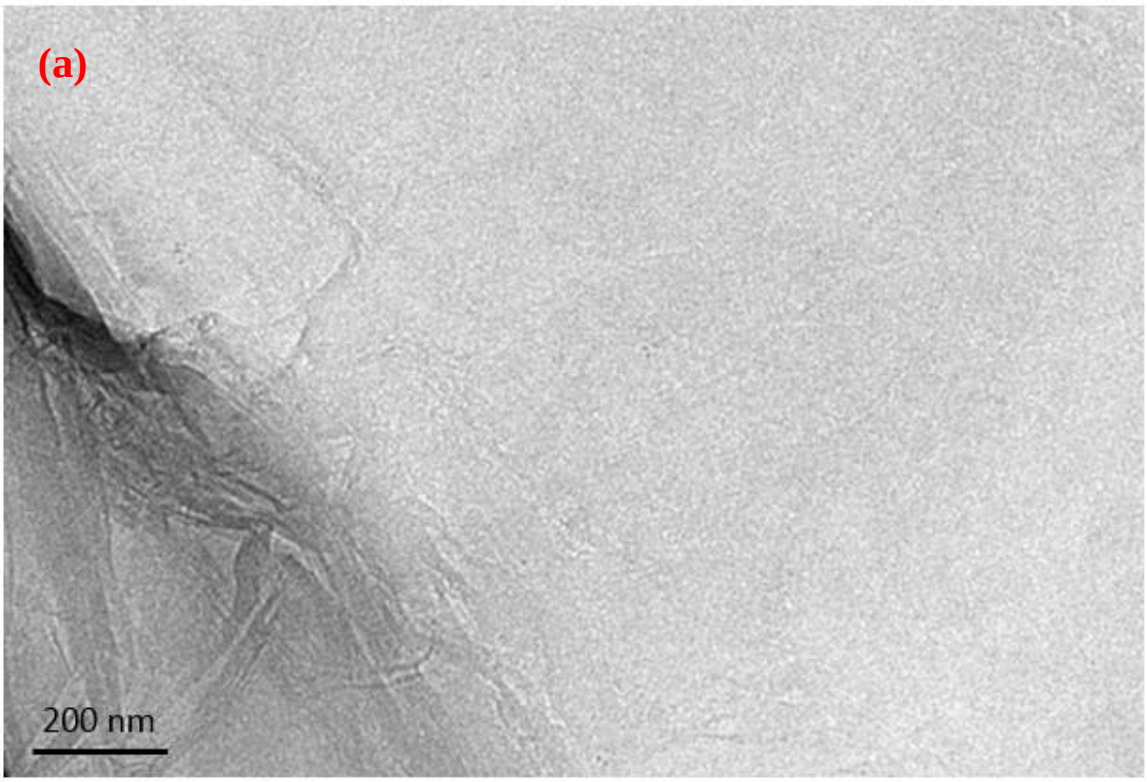

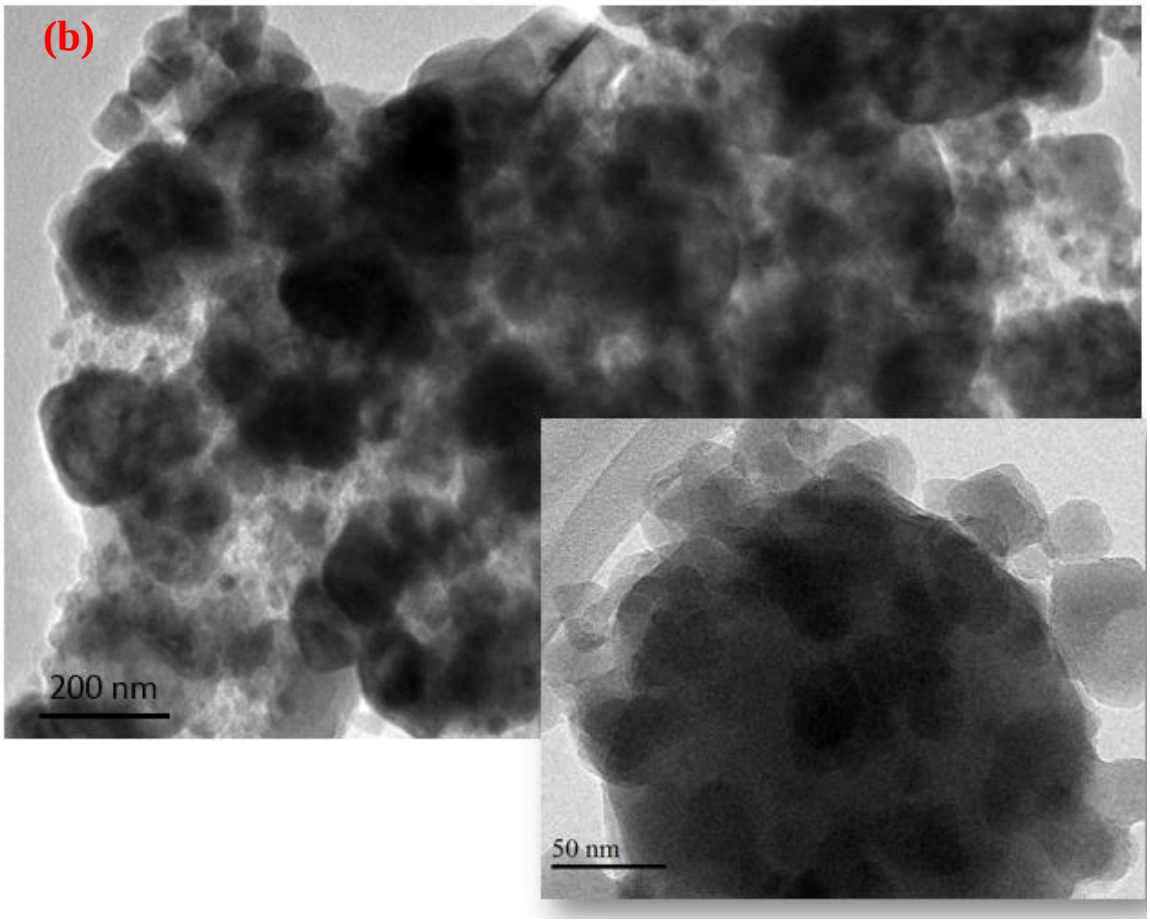

Figure 11 TEM of (a) graphene and (b) AlMoGNi

To study morphology and the chemical compositions of the AlMoNi and AlMoGNi catalysts, SEM/EDX analysis was conducted and the obtained results were presented in Figure 10. The SEM images of the prepared catalysts showed that the surface of AlMoGNi catalyst is smoother and the respective catalytic nanoparticles were distributed more uniformly than the corresponding ones in AlMoNi catalysts. Generally, larger surface area leads to a better nanometals dispersion with smaller sizes. As proven by N_2-physisorption analysis, the AlMoGNi has a noticeably larger surface area than AlMoNi, resulting in a better nanoparticles dispersion and this supports the H_2-TPR conclusion. The EDX

analysis of AlMoNi showed the presence of Al, O, Mo and Ni elements while AlMoGNi contained, in addition to those elements, carbon because of doped graphene.

The graphene and AlMoGNi catalysts were investigated using TEM analysis, as shown in Figure 11. The images for the used graphene indicated that it has a nontransparent surface with thin triples, as shown in Figure 11a. TEM images for AlMoGNi catalysts with resolution of 200 nm and 50 nm were shown in Figure 11b. It can be noticed that the active nanoparticles arrange closely and have high dispersion on the modified support due to the better metals-support interaction which confirm the TPR analysis results.

4.3.6 ICP-MS

The active metal compositions of the prepared supported bimetallic (Mo and Ni) catalysts were confirmed using ICP-MS. Molybdenum represented around 14.5 % while nickel represented around 4.6 % in the prepared catalyst samples, as shown in Table 4.

Table 4 ICP-MS results of the prepared catalysts

Catalyst	Mo (%)	Ni (%)
AlMoNi	14.3	4.8
AlMoGNi	14.5	4.6

4.3.7 FT-IR

FTIR analysis was conducted to reveal the function groups that are presented in the prepared catalysts and the obtained spectrum were shown in Figure 12. The characteristic peaks observed at ~947 and 740 cm^{-1} are associated to the fundamental vibrational modes of Mo=O while the peak at about 600 cm^{-1} is attributed to Al-O bending mode[131]. A

broad peak at about 3450 cm^{-1} and another peak at 1640 cm^{-1} were observed for both prepared catalysts and can be associated to O–H stretching and H– O–H, respectively[132]. This showed that the atmospheric moisture was adsorbed on the surface of the prepared catalysts. Unlike AlMoNi catalyst spectrum, AlMoGNi spectrum showed some different features which are two peaks at 2920 and 2850 cm^{-1}, indicated the symmetric and asymmetric $–CH_2$ stretching vibrations, respectively, in the doped graphene [133].

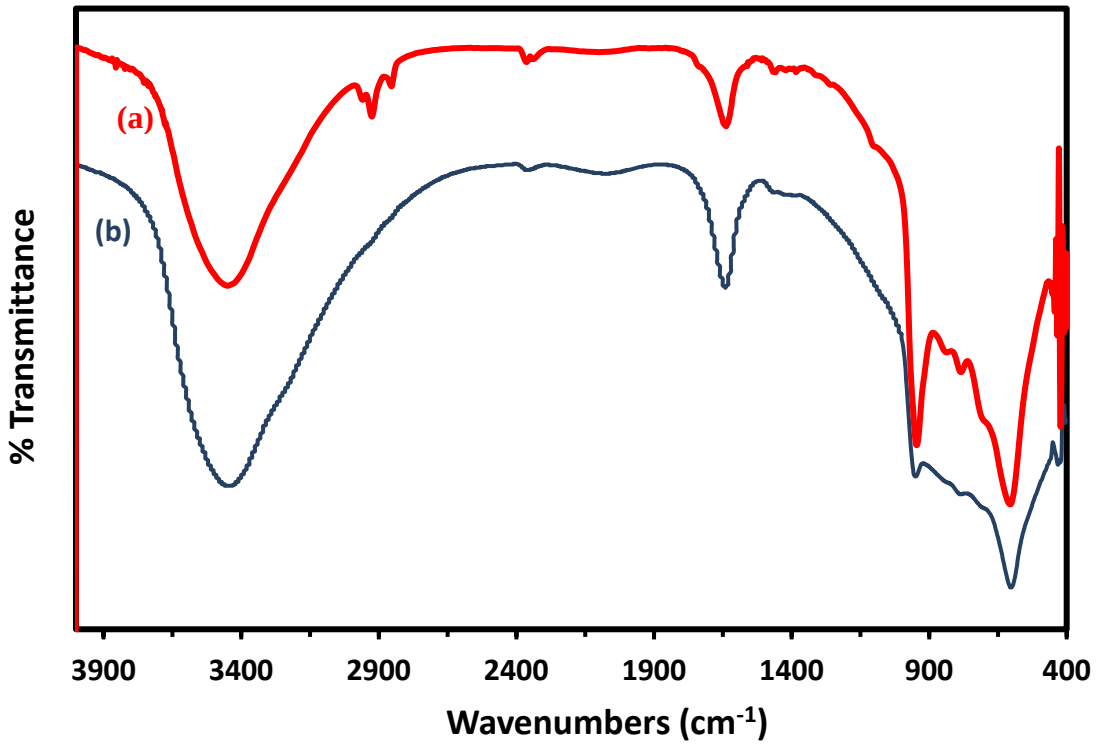

Figure 12 The FTIR spectrum of (a) AlMoGNi, and (b) AlMoNi

4.3.8 HDS Catalytic Activity of the Catalysts

The HDS catalytic performance of AlMoNi and AlMoGNi catalysts were evaluated and the removal percentage of the sulfur were related to the reaction time, as shown in Figure

13. The reactions were conducted in a batch reactor with 300 ^{o}C, 53 bar hydrogen partial pressure. 0.6g of each catalyst was used to desulfurize DBT in a decalin solvent as a model fuel which contains 600 ppm-S as an initial concentration. It can be noticed that AlMoGNi catalyst has a higher sulfur removal percentage compared to AlMoNi catalyst in the reaction time points, indicating that doping GNi has enhanced the HDS catalytic performance of the catalyst. The AlMoGNi catalyst was able to achieve 99% sulfur removal (11 ppm-S) within 5 hours reaction time compared to 84.2% sulfur removal (95 ppm-S) using AlMoNi catalyst in the same operating conditions.

The better catalytic activity of AlMoGNi catalysts can be attributed to the physico chemical characteristics of the modified catalysts. N_2-physisorption analysis of the prepared catalysts showed that the specific surface areas of AlMoGNi catalysts, especially the mesopore surface area, are considerably larger than that of AlMoNi catalysts, which leads to a better and more uniform distribution of active nanometals. The better dispersion of AlMoGNi nanoparticles was demonstrated by SEM images and H_2-TPR analysis. Also, NH_3-TPD analysis indicated that the AlMoGNi catalyst has more acidity than the AlMoNi catalyst, which means it possesses active sites with higher affinities to adsorb and desulfurize the feed more efficiently and better sulfur removal takes place on active sites. All these factors enhanced the HDS catalytic activity of the GNi doped catalysts compared to the conventional alumina-based catalysts.

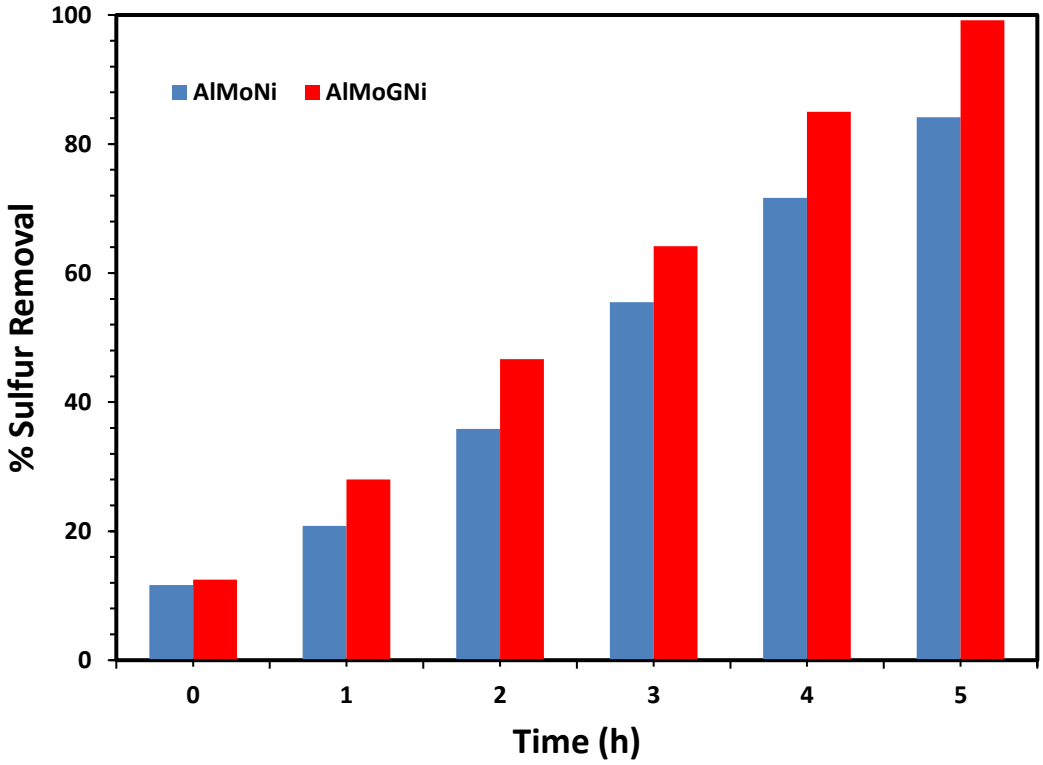

Figure 13 HDS catalytic activity of the prepared materials

4.3.9 HDS Reaction Mechanism

The HDS reaction of DBT over AlMoGNi have two possible pathways to occur, as shown in Figure 14. The first pathway is the hydrogenolysis pathway (DDS) and the second one is the hydrogenation desulfurization pathway (HYD). DDS occurs through σ adsorption of the DBT molecule via the sulfur atom, and HYD proceeds through π adsorption of the reactant via the aromatic system.

In the DDS mechanism, the sulfur removal from DBT is achieved by a direct C-S bond cleavage, producing biphenyl (BP) compound and H_2S as a final product [134]. In the HYD mechanism, one of the DBT aromatic rings is hydrogenated, yielding

tetrahydrodibenzothiophene (THDBT) and/or hexahydrodibenzothiophene (HHDBT) as intermediate products. These intermediates are very reactive intermediates and are difficult to isolate for detection. The second step includes desulfurization of HHDBT and/or THDBT, producing cyclohexylbenzene (CHB) and H_2S as final products.

GC-MS was used to identify the HDS products and to predict the reaction pathways by analyzing the obtained sample after 6h reaction time over AlMoGNi catalyst. The overall gas chromatogram of HDS of DBT was shown in Figure 15a. One peak corresponding to unreacted DBT was identified in the analyzed product sample, as shown in Figure 15b. BP and CHB products were reorganized by the two peaks in Figure 15 c,d, respectively. This showed that the HDS of DBT over AlMoGNi catalyst occurred via DDS and HYD reaction pathways.

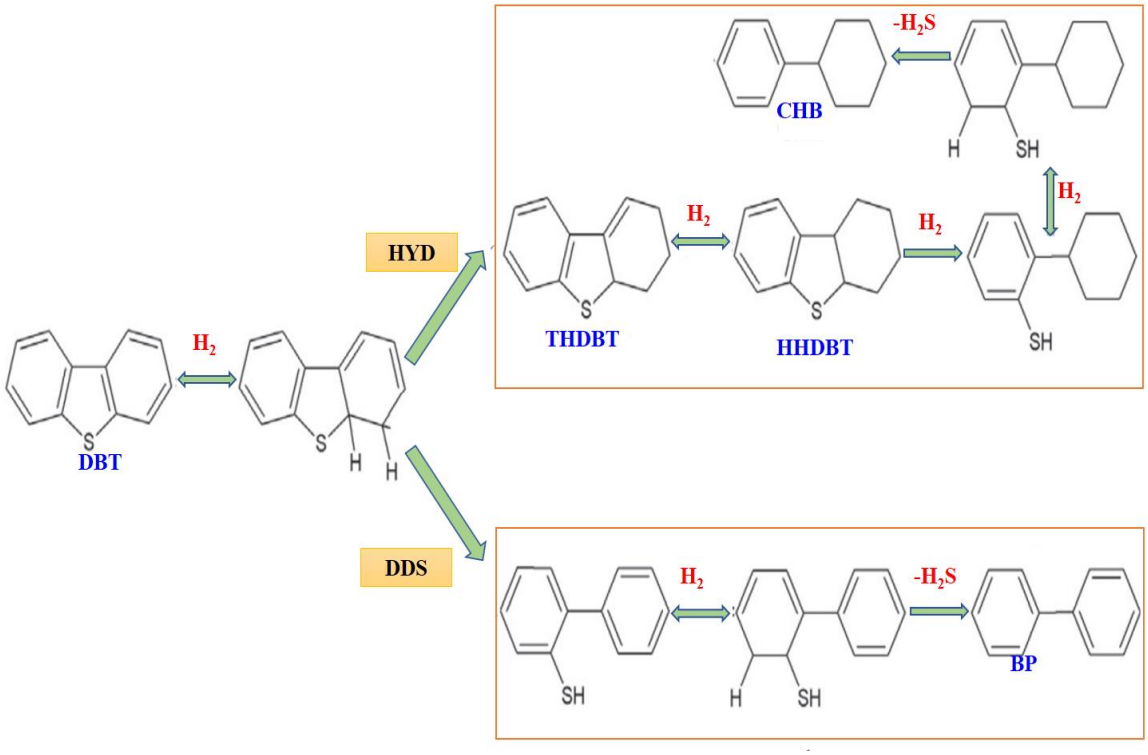

Figure 14 HDS of DBT reaction pathways over AlMoGNi catalyst

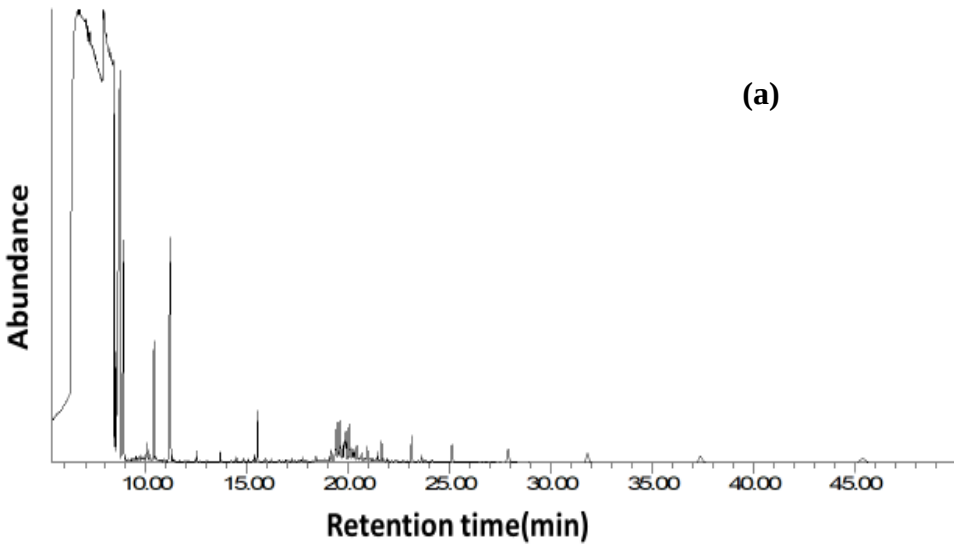
(a)
Abundance
10.00
15.00
20.00
25.00
30.00
35.00
40.00
45.00
Retention time(min)

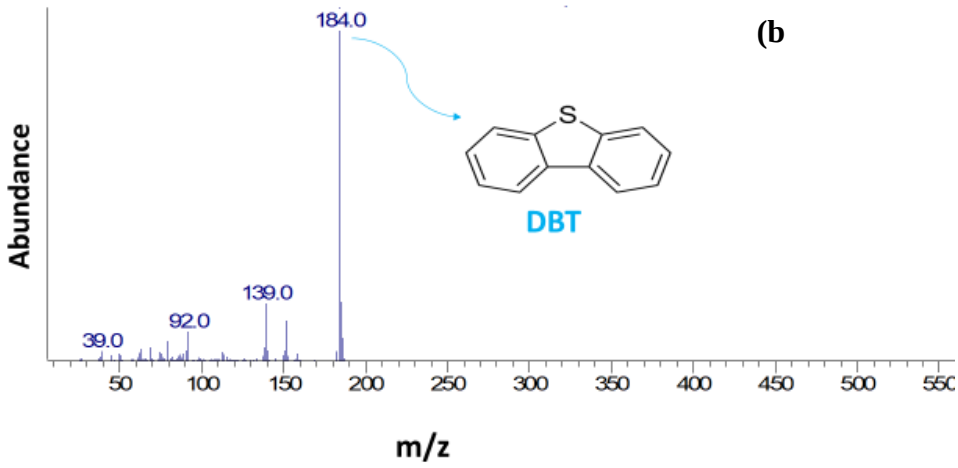
(b
184.0
S
DBT
Abundance
139.0
92.0
39.0
50
100
150
200
250
300
350
400
450
500
m/z

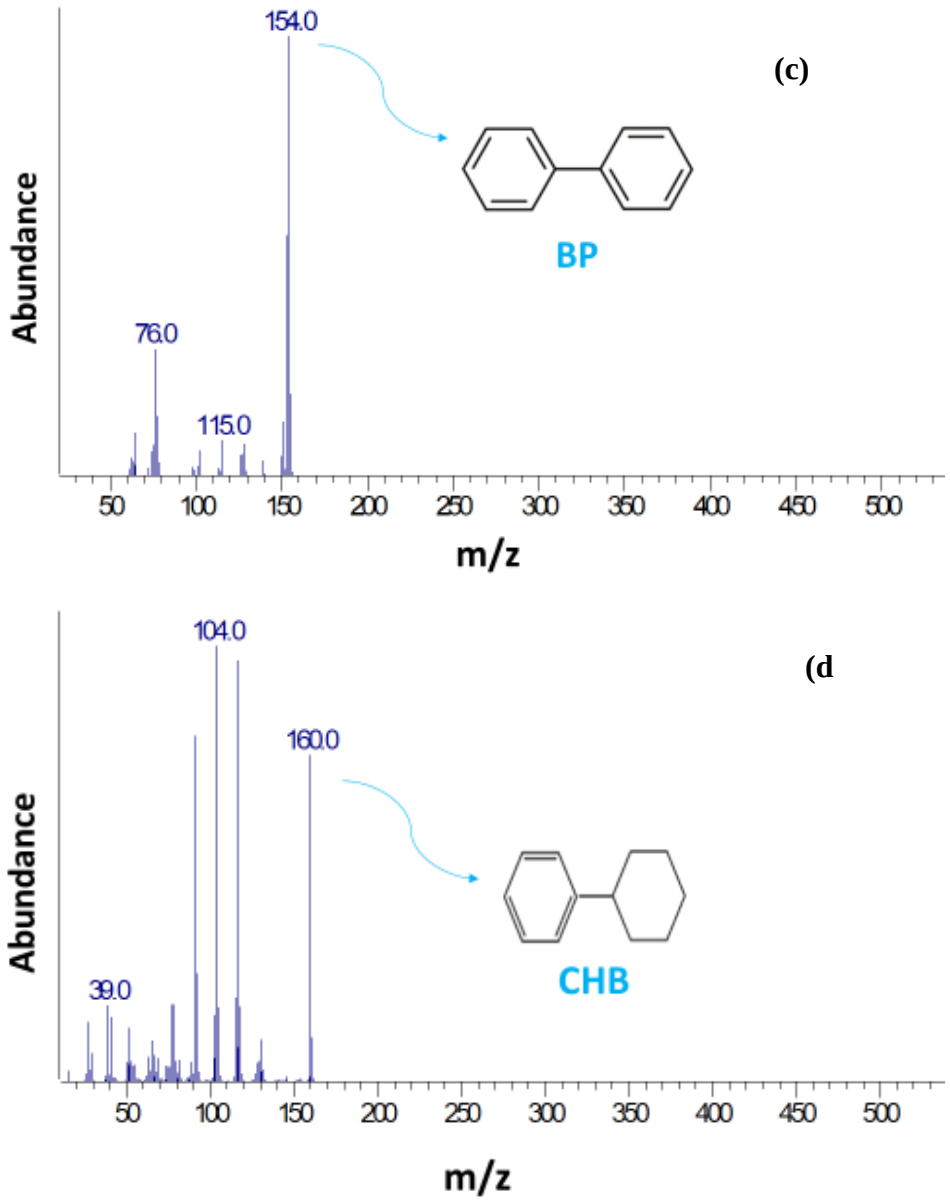

Figure 15 (a) Gas Chromatogram of HDS products (b) Part of GC-MS corresponding to DBT product (c) corresponding to BP product and (d) corresponding to CHB product.

4.4 Conclusion

Alumina-supported Mo catalyst was doped with Ni nanometals supported on graphene to form AlMoGNi catalyst. This catalyst was successfully synthesized, characterized and tested for the HDS of DBT and compared with the corresponding AlMoNi catalyst. The

experimental results showed that AlMoGNi catalyst has a better catalytic activity in removing sulfur from liquid fuel compared to the AlMoNi catalyst. AlMoGNi catalyst achieved 99% sulfur removal within 5h reaction time compared to 84 % with AlMoNi catalyst under similar reaction conditions. The enhanced textural characteristics, good surface acidity, and high metals dispersion were the important elements that boost AlMoGNi catalytic activity. As showed by GC-MS analysis, the reaction over AlMoGNi catalyst occurred through DDS and HYD pathways.

CHAPTER 5

A Novel Alumina-CNF Composite as a Support for Molybdenum-Cobalt Catalysts

Abstract

Alumina-CNF nanocomposite support for MoCo catalyst (AlCNFMoCo) was prepared, characterized and tested for hydrodesulfurization of dibenzothiophene in liquid fuels. The AlCNFMoCo catalysts were compared with the corresponding conventional alumina-supported catalysts (AlMoCo). The alumina-CNF composite was prepared by sol-gel method and then loaded with Mo and Co nanoparticles by the incipient wetness impregnation method. The different types of the catalysts were characterized by N_2-physisorption, temperature programmed analysis by reduction, X-ray diffraction, scanning electron microscope, energy-dispersive X-ray spectroscopy etc. The BET surface areas of AlMoCo and AlCNFMoCo were 166 and 200 (m^2/g), respectively. The catalysts were evaluated by HDS reaction in a batch reactor at the following operating conditions: temperature of 300 ^oC, 55 bar H_2 partial pressure and 0.5g of the prepared catalyst. The model fuel was prepared using decalin as a solvent with 550 ppm-S. 97% and 85.8% sulfur removal were obtained using AlCNFMoCo and AlMoCo catalysts, respectively, indicating that doping CNF into γ-Al_2O_3 support has boosted the catalytic activity to desulfurize liquid fuels.

5.1 Introduction

The diesel, oil, and gasoline usually contain a considerable amount of compounds which contain sulfur, and that generate SO_X gases. These gases pollute the environment and lead to human health problems. From the petrochemical point of view, SO_X gases reduce the efficiency of the plant units and cause a severe corrosion to the reactors, and the storage and export vessels[95]. Thus, stricter environmental regulations and constraints have been enforced on the oil industry to minimize the sulfur content in the refinery products as much as possible and to meet the new fossil fuel quality specifications[94].

Different methods have been applied to reduce the sulfur percentage in the crude oil and its fractions, such as gasoline, diesel and jet fuel. These methods include hydrodesulfurization (HDS), extractive desulfurization (EDS), oxidative desulfurization (ODS), adsorptive desulfurization (ADS) and biodesulfurization (BDS).

HDS involves a reaction between a liquid fuel and a hydrogen stream on heterogeneous catalysts at high temperature and pressures [135–137]. EDS include a mixing of the fuels with suitable solvents and subsequent separation to extract the organosulfur species[93,138,139]. ADS don’t need a high temperature and the organosulfur compounds are successfully removed by physisorption on the surface/matrix of the adsorbent material [140–143]. ODS involves the oxidation of the organosulfur compounds using oxidants and then the subsequent separation of the resulting sulfoxides or sulfones through extraction with a suitable solvent [20,144,145] and BDS include the use of microorganisms that have the inherent capacity to transform/utilize the organosulfur compounds especially through metabolism[146–148].

However, HDS is the most used technique in oil refinery processes due to its effectiveness and practicality compared to other techniques [12] . However, the HDS process depends highly on the performance and stability of the used catalysts. Thus, the academic and industrial communities are trying to develop effective catalysts and to improve the available ones to ensure the effective removal of sulfur to conform with the required minimum levels.

Catalysts consisting of active phase Mo or MoS_2, then promoted with Ni or Co and supported on gamma-alumina are used widely for the HDS process in oil refinery plants [99,100,149]. The catalyst support plays a critical role in the stability and performance of the used catalysts in the HDS process since it provides the required surface area for the active sites to be dispersed. Different materials have been investigated as a support for HDS catalysts including zeolites[13,89], carbon [82,101,150], zirconia [108,109], titania [105,106], and silica [78,151].

However, alumina is the most widely used as a support material for the HDS process catalysts because of its mechanical strength which makes the catalyst stable under the harsh reaction conditions of the HDS process. Also, the alumina structure includes acidic sites and has a high surface area and good porosity. However, many researchers reported that alumina has a strong interaction with transition metal oxides which impedes complete sulfidation, ultimately reducing the HDS performance of the catalysts.

Recently, investigations have focused on nanofilamentous carbons (NC), including carbon nanofibers (CNF) and carbon nanotubes as a support for the HDS process. The reported results indicated that the NC-supported catalysts, with a large surface area, showed better

activity for HDS compared to the conventional alumina-supported catalysts [126,152,153]. In spite of that, alumina is still of interest due to its mechanical characteristics. Thus, researchers are trying to develop effective catalysts combining the high surface area of NC with the mechanical strength of alumina, in addition to using different methods to improve the alumina-based catalysts for the hydrotreatment process. One of these methods is to combine the alumina with other support materials such as activated carbon, zeolite, SiO_2, ZrO_2 and TiO_2 to obtain the positive characteristics of both combined systems [85,86,154].

In this contribution, a novel carbon-nanofiber doped alumina (AlCNF) was designed and investigated as a support for the MoCo catalyst. The AlCNFMoCo catalyst was evaluated for its HDS activity and it showed superior performance over the MoCo catalysts supported on alumina (AlMoCo). The prepared materials were characterized by several techniques including FT-IR, XRD, TGA, BET, TPR, and SEM-EDX, in order to get insight into their structural and morphological properties and how they affect the catalytic activity performance of the prepared catalysts.

5.2 Catalytic Evaluation

The HDS activity of the catalysts was evaluated using a batch reactor, model 4848B, which was purchased from the Parr Instrument Company. The HDS system is composed of a reactor, a hydrogen gas supplier, gas controller, and the valves for controlling the input and output samples, as shown in Figure 5. The HDS reaction occurred at T = 300 °C and 55 bar hydrogen partial pressure. Around 0.5 g of the catalyst was inserted in the reactor vessel with 100 ml of the model fuel containing DBT at an initial concentration of 550 ppm-S in decalin as a solvent model fuel. When the temperature of the reaction was increased up to 300 °C, the first sample was collected and considered as the zero point. Then, after one

hour of the reaction, a sample was collected by a manual valve and the reaction was monitored for 6h. Finally, the concentrations of sulfur in the collected samples were detected by gas chromatography employing sulfur chemiluminescence detection (GC-SCD); and product identification was achieved with gas chromatography mass spectrometry (GC–MS). Different reactions were conducted with AlMoCo and AlCNFMoCo catalysts.

5.3 Results and Discussion

5.3.1 Surface and Textural Properties

The N_2 adsorption-desorption isotherm curves of AlMoCo and AlCNFMoCo were shown in Figure 16a. The isotherm curves of both catalysts resemble a type IV isotherm with micro/mesopores contributions in the adsorption-desorption processes. The N_2 uptake at small values of relative pressure indicates the presence of micropores, while the hysteresis loop at high values of relative pressure indicates the mesopores existence in the prepared catalysts.

Table1 contains the textural characteristics of the prepared catalysts and it can be observed that the AlCNFMoCo catalyst has a higher BET surface area, mesopore surface area, micropore surface area, total pore volume and micropore volume than the AlMoCo catalyst. Figure 16b hows the pore size distribution of the AlCNFMoCo and AlMoCo catalysts, indicating that both catalysts have a mesoporous character with close dominant pore diameter values of 6.24 and 7.15 nm, respectively. Therefore, the CNF enhances most of the AlMoCo textural properties without severe penalization of the average pore diameter.

For further investigation of the CNF effects on the textural properties, the hierarchy factor (HF) for both materials was calculated. The hierarchy factor was calculated using equation (1) as:

$$HF = (V_{micro}/V_{total}) * (S_{meso}/S_{BET}) \quad (1)$$

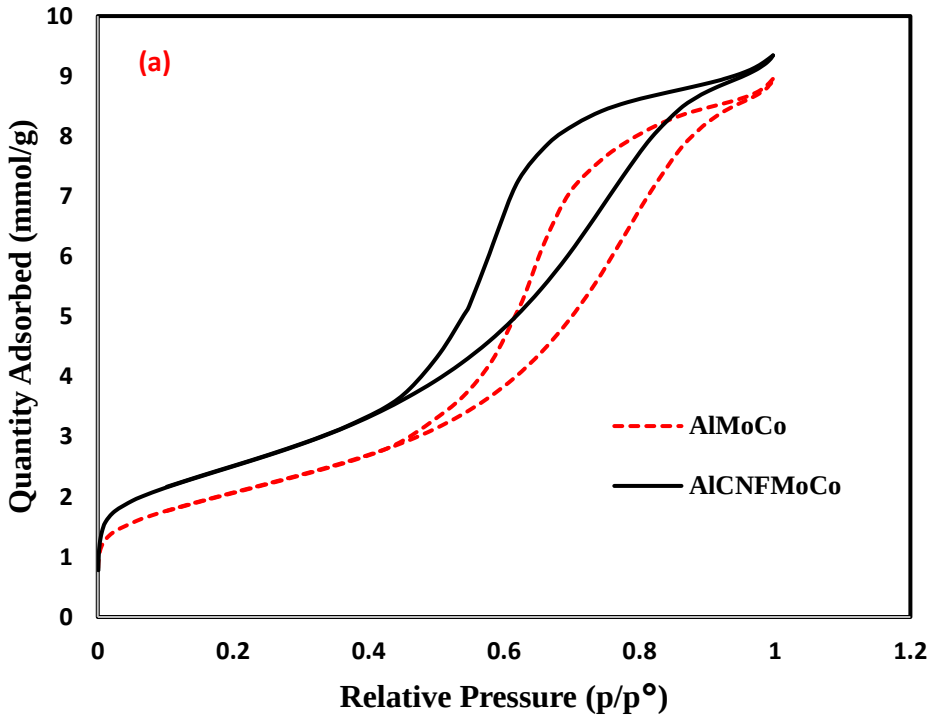

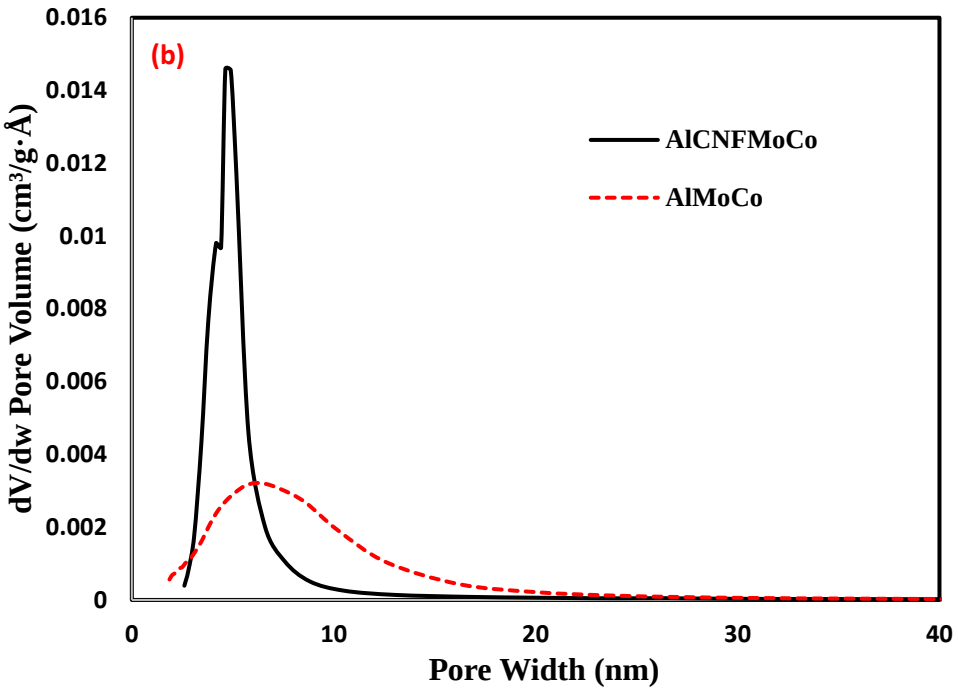

Figure 16 (a) N_2 adsorption-desorption isotherm (b) and the pore size distribution of the prepared catalysts

By substituting the textural parameter values into the equation (1), the HF values were obtained for AlMoCo and AlCNFMoCo, as shown in Table 5. The results show that AlCNFMoCo has a higher HF value than AlMoCo, indicating the possibility that it has a higher adsorption efficiency[125]. As shown in Figure 16a, the quantity adsorbed-desorbed by AlCNFMoCo at any relative pressure is higher than the quantity adsorbed-desorbed by AlMoCo, which supports the HF conclusion.

Table 5 Properties of the prepared catalysts obtained from N_2 physisorption

Catalysts	S_{BET}[a]	S_{Meso}[b]	S_{Micro}[c]	V_{micro}[d]	V_{total}[e]	APD[f]	HF*
AlMoCo	166	155	11	0.0044	0.3055	7.15	0.013

AlCNFMoCo	200	177	23	0.0096	0.3179	6.24	0.027

[a] BET Surface area (m^2/g), [b] Mesopore surface area (m^2/g), [c] Micropore surface area (m^2/g), [d] Micropore volume (cm^3/g), [e] Total pore volume (cm^3/g), [f] Average pore diameter (nm), *Hierarchical factor (HF).

5.3.2 H_2-TPR

H_2-TPR analysis was used to investigate the interaction between the active species and the two different support materials including γ-Al_2O_3 and AlCNF supports by studying its reduction behavior using H_2 gas. Figure 17 exhibited the H_2-TPR profiles of the prepared catalysts. Both AlMoCo and AlCNFMoCo catalysts have two reduction peaks within the temperature range of 410- 560 °C and one reduction peak within the temperature range of 700–770 °C.

The first reduction peaks in the temperature range of 410-560 °C is typically assigned to the reduction (Mo^{6+}-Mo^{4+}) of polymeric octahedral Mo species bonded to surface of the support weakly. The second reduction peak in the temperature range of 700-770 °C is associated with a reduction (Mo^{4+}-Mo^{0}) of polymeric octahedral Mo and isolated tetrahedral Mo species interacted with the support strongly.

The reduction peaks temperatures in TPR profile indicate the metal-support interaction in the prepared catalysts. It has been reported that reduction temperature at higher values showed a high interaction between the active species and the support, that reduce the metals dispersion on the catalysts and reduce its catalytic activity. As shown in Table 6, the peak locations at a low temperature of the AlCNFMoCo have lower values compared to AlMoCo, which means that it has a better metals-support interaction. Thus, the AlCNFMoCo catalysts have a better metal dispersion which increases its HDS catalytic

activity. Also, the results showed that the active speices of AlCNFMoCo catalytsts are much easier to be reduced compared to those in the AlMoCo catalyts, resulting in fast DBT conversion and products with less sulfur contents.

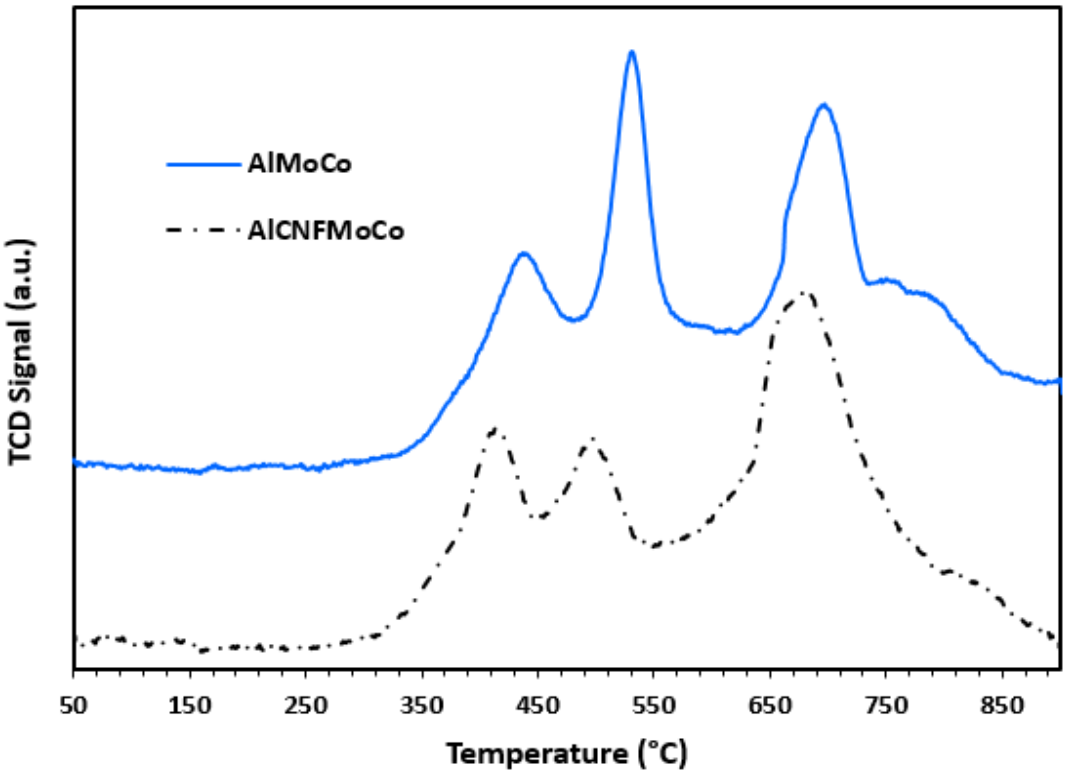

Figure 17 H_2-TPR curves of AlMoCo and AlCNFMoCo catalysts

Table 6 H_2-TPR results of AlMoCo and AlCNFMoCo catalysts

Catalyst	H_2-TPR		
	Temperature at Maximum (°C)	Quantity (mmol/g)	Total quantity (mmol/g)

AlCNFMoCo	413 496 738	0.1715 0.1574 1.4757	1.084
AlMoCo	435 530 696	0.1638 0.3911 0.4522	1.007

5.3.3 XRD

Fig. 18 showed the XRD patterns of the prepared catalysts after calcination at 350 °C. As shown in the XRD pattern of the CNF, the most noticeable feature is the graphite (002) diffraction peak, positioned at around 26◦. Other peaks related to the CNF are the (100) and (101) reflections, in the region between 42◦ and 45◦. Another low intensity line is the (004) near 55◦. The diffraction patterns of the AlMoCo show the characteristic peaks of alumina and MoCo confirming the presence of CoMoOx (JCPDS 00-021-868), and crystalline molybdenum oxide (JCPDS 01-072- 0527). The introducing of cobalt and molybdenum oxides affords a peak at 26.6◦ which can be attributed to monoclinic - CoMoO4. In addition to other characteristic peaks at 2θ = 34°, 39°, 46.5°, and 66°, the XRD pattern of the AlCNFMoCo catalysts shows the CNF characteristic peaks. The difference between the XRD patterns of AlMoCo and the AlMoCoCNF catalysts is the graphite (002) diffraction peak at ~ 26°, which slightly overlaps with the Al peak at 26.6°.

This indicates the success of the CNF embedding within the AlCNF support.

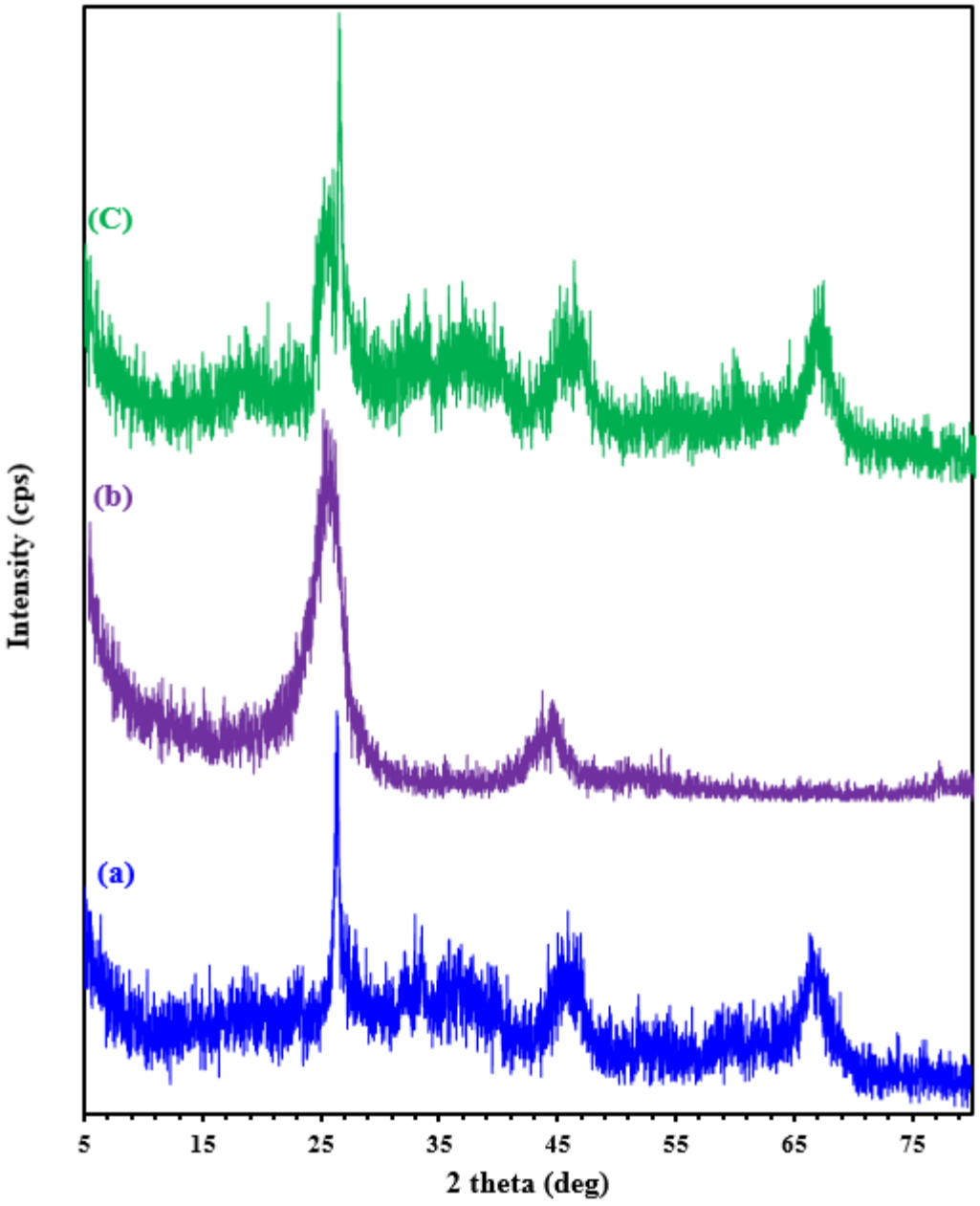

Figure 18 XRD pattern of (a) the AlMoCo (b) CNF (c) and AlCNFMoCo catalysts

5.3.4 SEM/EDX and TEM

The morphology of the prepared catalysts and the elemental compositions were investigated by SEM images and EDX analysis. As shown in Figure 19b, the morphology of the AlCNFMoCo catalyst powder contains a small number of carbon fibers, confirming the presence of CNF with a small diameter as shown in TEM image. The SEM images showed that the metal nanoparticles were distributed uniformly on the surface of the AlCNF composite support, resulting in minimizing the agglomeration. These CNFs provide a high surface area in which the metal nanoparticles to be dispersed increase the available active sites of the prepared catalysts. The EDX analysis of the AlCNFMoCo catalysts revealed the existence of Al, O and C elements due to the use of the AlCNF as a composite support for the prepared catalyst, Figure 19b. Also, it showed the presence of the catalyst metals Mo and Co with 13.52 wt% and 4.83 wt%, respectively.

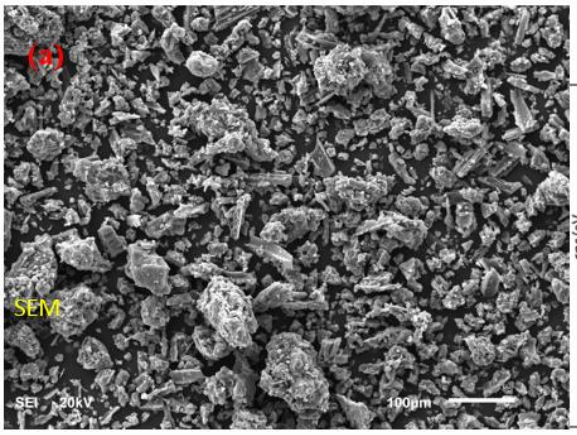

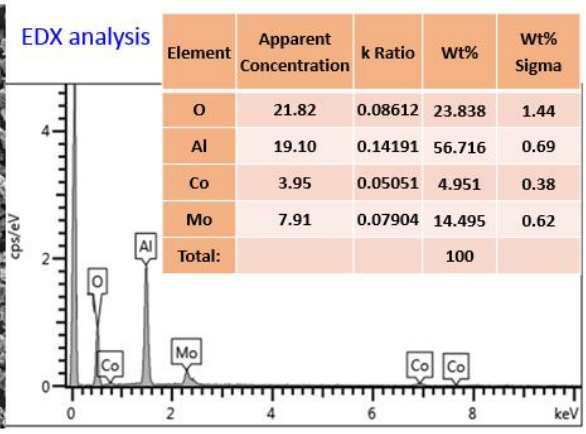

Element	Apparent Concentration	k Ratio	Wt%	Wt% Sigma
O	21.82	0.08612	23.838	1.44
Al	19.10	0.14191	56.716	0.69
Co	3.95	0.05051	4.951	0.38
Mo	7.91	0.07904	14.495	0.62
Total:			100	

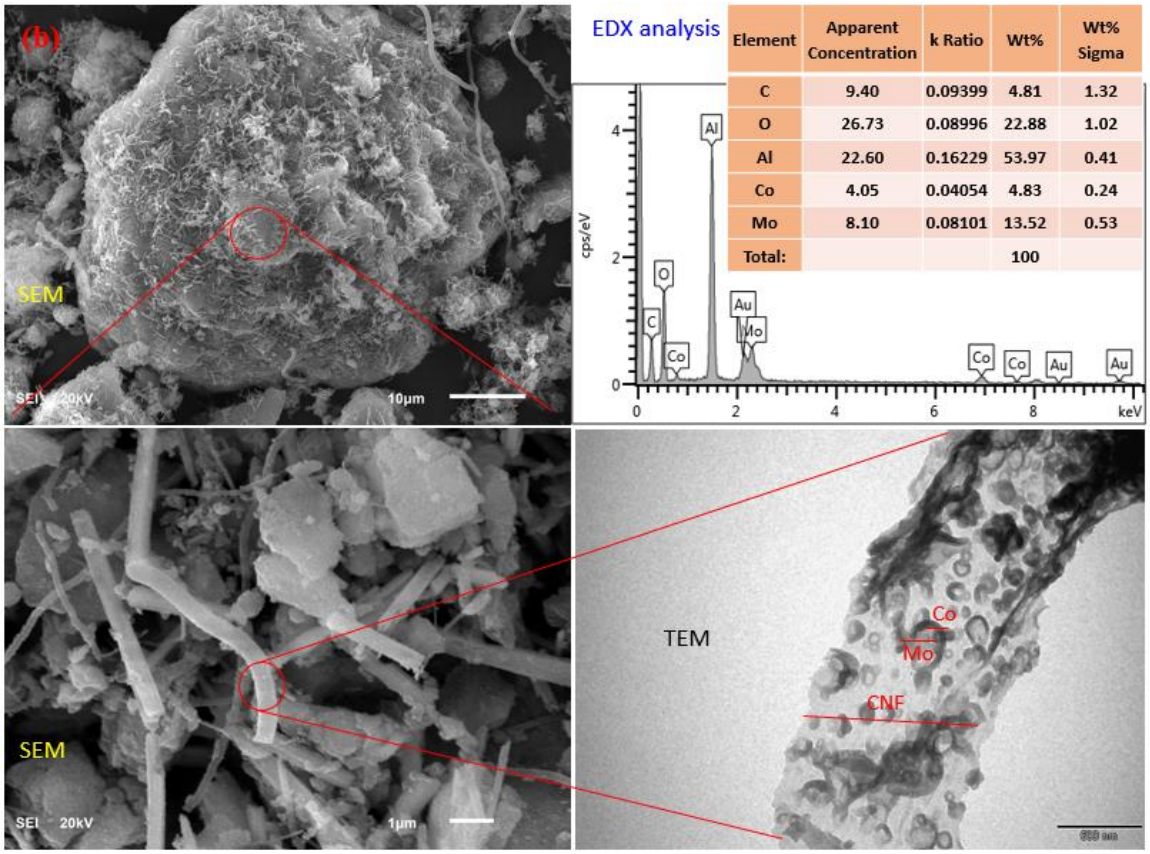

Figure 19 (a) SEM image and EDX analysis of AlMoCo, (b) SEM images, EDX analysis and TEM image of AlCNFMoCo catalyst.

5.3.5 FT-IR

The FTIR spectra of the AlCNFMoCo and AlMoCo catalysts were obtained in order to reveal the functional groups on the surface of the prepared materials. As shown in Figure 20, the band around 550-870 cm^{-1} can be associated with the symmetric and asymmetric MoO terminal stretches. The characteristic peaks observed in the FT-IR spectrum of Mo=O at ~988, 878 and 634 cm^{-1} were attributed to the fundamental vibrational modes of Mo=O. The dominion band at ~820 cm^{-1} is associated with the vibration of the Mo-O-Mo bridging bonds. It should also be noticed that there could be an overlap of the characteristic peaks of Mo=O with that of the alumina which appeared at ≈741 and ~641 cm^{-1} (Al-O bands).

The broad peaks at 550-900 suggested that MoCo were highly dispersed on the alumina support. In the IR spectrum of AlMoCo, the broad peak at around 3400 cm^{-1} is indicative of the presence of –OH groups on the surface (OH stretching–Al–OH) and the peak at 1637 cm^{-1} is due to –OH bending [155]. After doping with CNF, the peak appears at 2920 and 2850 cm^{-1} which are characteristics of the asymmetric and symmetric $–CH_2$ stretching vibrations in the CNF [156].

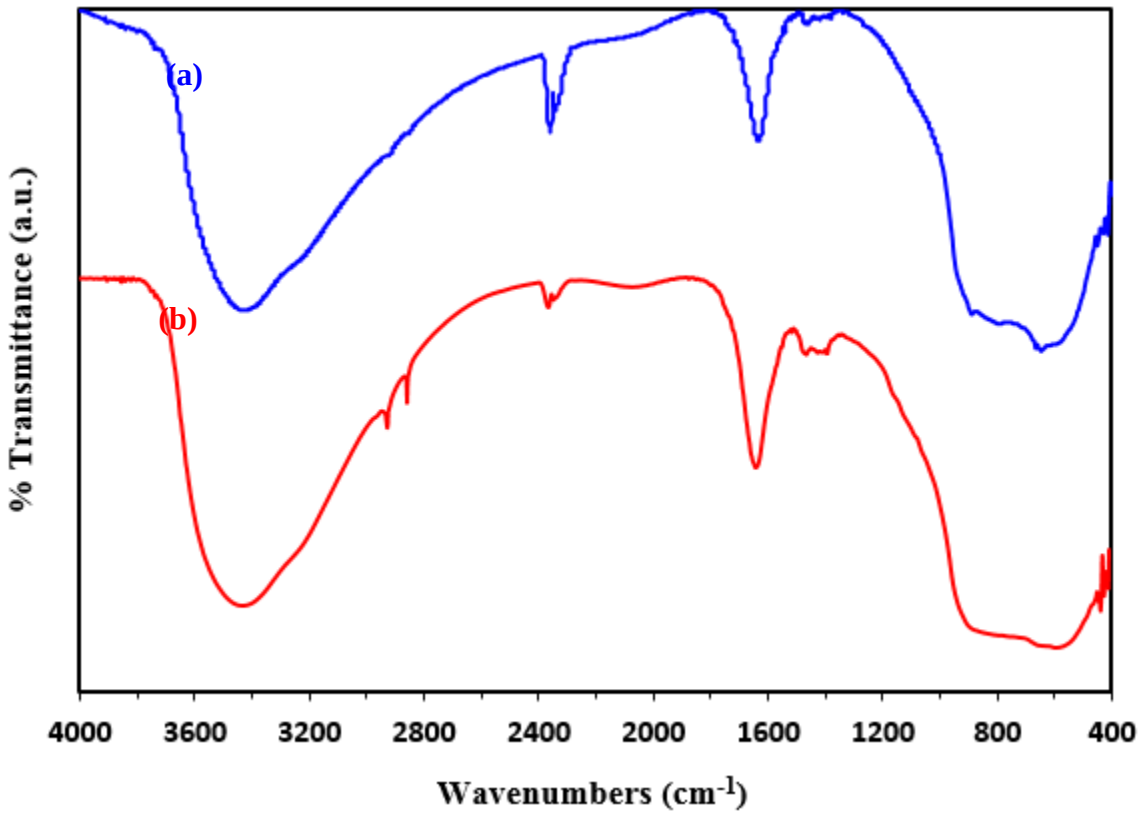

Figure 20 The FTIR spectrum of (a) the prepared catalysts; AlMoCo (b) AlCNFMoCo.

5.3.6 TGA

Thermal stability is another important factor to evaluate the workability of the catalysts at high temperatures. The TGA analysis curves of the AlMoCo and AlCNFMoCo indicated

that both have a good thermal stability, which is not affected by introducing CNF. From the curves, Figure 21, it can be observed that there is a sharp weight loss below 250 °C at amounts of 10wt% and 13.5wt% for AlCNFMoCo and AlMoCo, respectively. This can be attributed to the desorption of the absorbed moisture. The decomposition of the water molecules occurs at low temperatures, as shown in the TGA curves since their binding with the support is very weak. Most of this water is bound in an OH form which matches with the FTIR results that signified the presence of the OH group on the surface of the prepared catalysts. The other weight loss for both catalysts accrued in a temperature range of (250-750 ˚C) and it was associated with the decomposition of the residual precursor. However, according to the TGA curves, the decomposition rate of AlMoCo is faster than the corresponding one in the AlCNFMoCo under the same testing conditions, indicating that the AlCNFMoCo catalysts have a better thermal stability than the AlMoCo catalysts. This can be attributed to the presence of CNF as a co-support in the AlCNFMoCo catalysts.

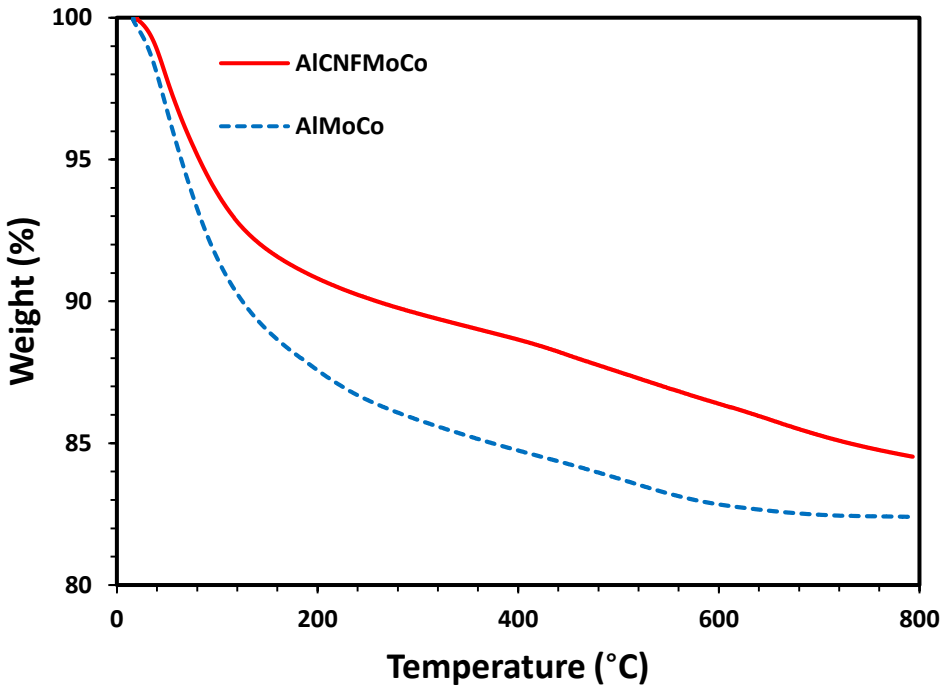

Figure 21 TGA curves of the AlMoCo and AlCNFMoCo catalysts

5.3.7 HDS Activity of Prepared Catalysts

Figure 22 presents the sulfur content removal as a function of the time reaction. It includes the AlCNFMoCo and AlMoCo catalytic activity towards desulfurization of the DBT in a decalin solvent as a model fuel. The operating conditions were 300 ^{o}C; 55 bar hydrogen partial pressure, catalyst amounts of 0.5g, and 100 ml of the model fuel. It can be observed that AlCNFMoCo has a better catalytic performance during the time reaction intervals compared with the AlMoCo catalyst. After 6 hours of reaction at a constant temperature of 300 ^{o}C, the AlCNFMoCo catalyst was able to achieve 97 % sulfur removal compared to 85.8% achieved by the AlMoCo catalyst.

One of the main factors that play a critical role in the catalytic activity is the textural properties of the used materials [12]. The HDS of DBT usually occur in the mesoporous structure rather than in the microporous structure over the prepared materials since the DBT is a relatively large molecule [11]. The mesopore surface area of the AlCNFMoCo is 177 (m^2/g) while the AlMoCo catalysts have a 154 (m^2/g) mesopore surface area at the same metal loading, indicating that the increase in the surface area was mainly due to the CNF-doping. Also, the adsorption/desorption efficiency of AlCNFMoCo is better than that of AlMoCo, as indicated by the results of the adsorption/desorption isotherms and the HF calculations. Notably, the CNF has improved the surface characteristics of the gamma-alumina support, leading to a higher performance in the HDS process of the AlCNFMoCo compared with the AlMoCo catalysts. These textural characteristics, including surface area and pore volume, lead to improved metal dispersion on the AlCNF support compared to an alumina support, as indicated by the TPR analysis, which in turn increases the catalytic activity of the prepared catalyst [157].

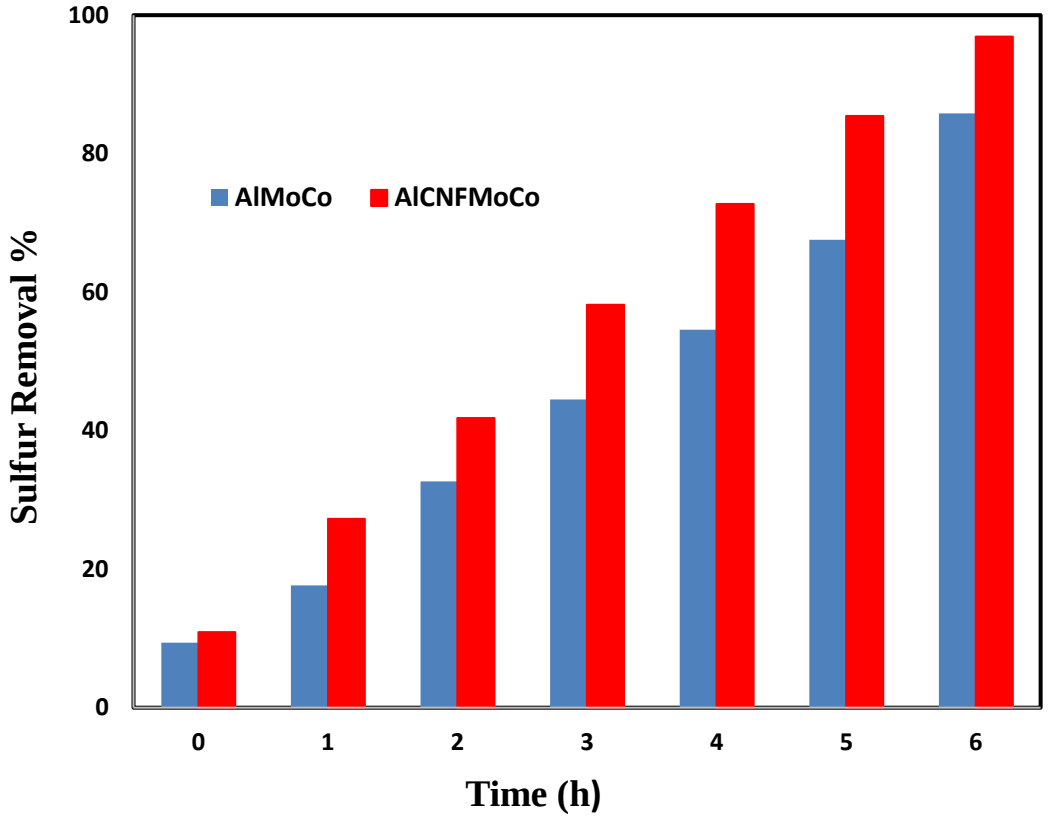

Figure 22 The catalytic activity of the prepared catalysts

5.3.8 HDS Reaction Mechanism

Generally, there are two main reaction mechanisms for the HDS process of DBT, namely, the hydrogenolysis pathway (DDS) and the hydrogenation desulfurization (HYD) pathway. In the DDS mechanism, the removal of the sulfur is is due to hydrogen, without abetting the DBT aromatic rings. In the HYD mechanisms, the aromatic rings are hydrogenated and then desulfurized.

The possible reaction mechanism for the HDS of DBT over the AlCNFMoCo catalysts is illustrated in Figue 23. In the DDS pathway, the removal of sulfur by direct C-S bond hydrogenolysis produces biphenyl (BP) which can be considered as the predominant

organic product in this pathway. Subsequently, the BP is hydrogenated to produce cyclohexylbenzene (CHB). By contrast, the hexahydrodibenzothiophene (HHDBT) or/and tetrahydrodibenzothiophene (THDBT) are the intermediate products of the main reaction in the HYD pathway mechanism. These intermediates are desulfurized to give a secondary product which is cyclohexylbenzene (CHB). In both mechanisms, bicyclohexyl (BiCh) is formed in trace amounts, which is the result of the hydrogenation of the CHB in a slow pattern.

GC-MS was conducted to reveal the reaction products in order to predict the mechanism pathway by analyzing samples of the HDS reaction products over the AlCNFMoCo catalyst. Peaks corresponding to the HDS of DBT are shown in Figure 24. As shown in Fig. 24a, the obtained GC-MS peaks for the products are quite complex since about 500 compounds are separated in every analysis. Also, the important peaks corresponding to the HDS products are in the low level of abundances. However, two peaks corresponding to biphenyl and bicyclohexyl were identified in Figure 24b, c, respectively. This indicates that the HDS reaction over the AlCNFMoCo catalysts has a DDS reaction mechanism.

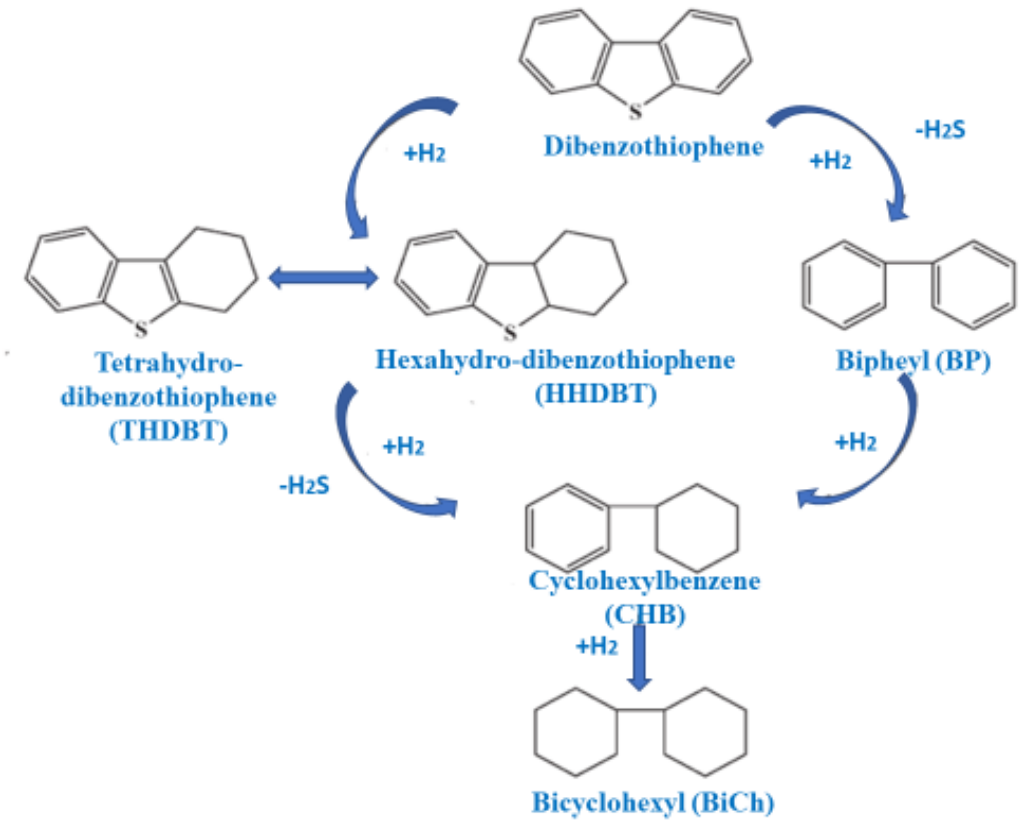

Figure 23 Possible pathways for the HDS of DBT at 300 °C in the presence of AlMoCo or AlCNFMoCo catalysts

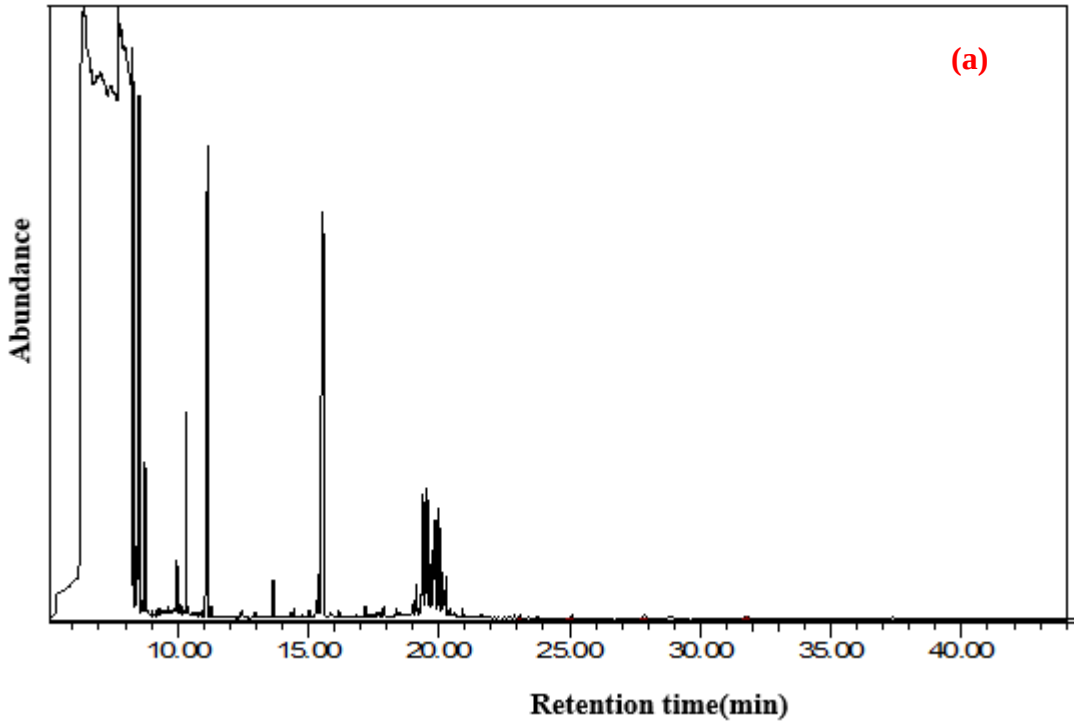
(a)
Abundance
10.00
15.00
20.00
25.00
30.00
35.00
40.00
Retention time(min)

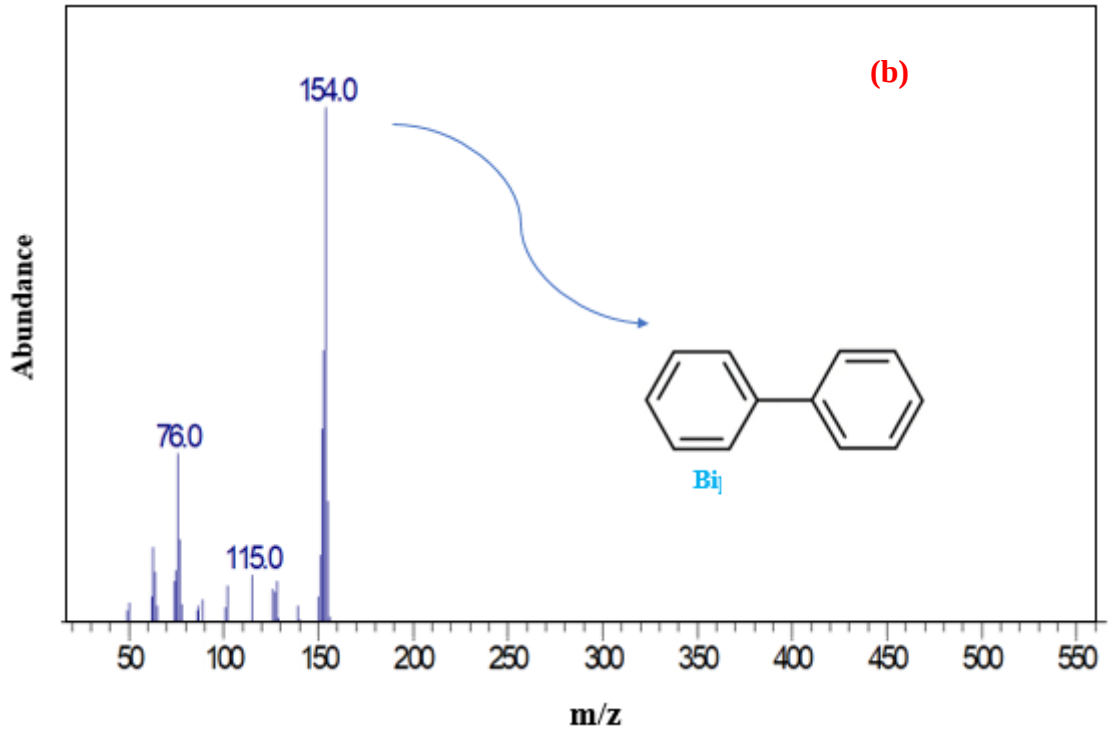
(b)
154.0
76.0
115.0
Abundance
50
100
150
200
250
300
350
400
450
500
550
m/z
Bi

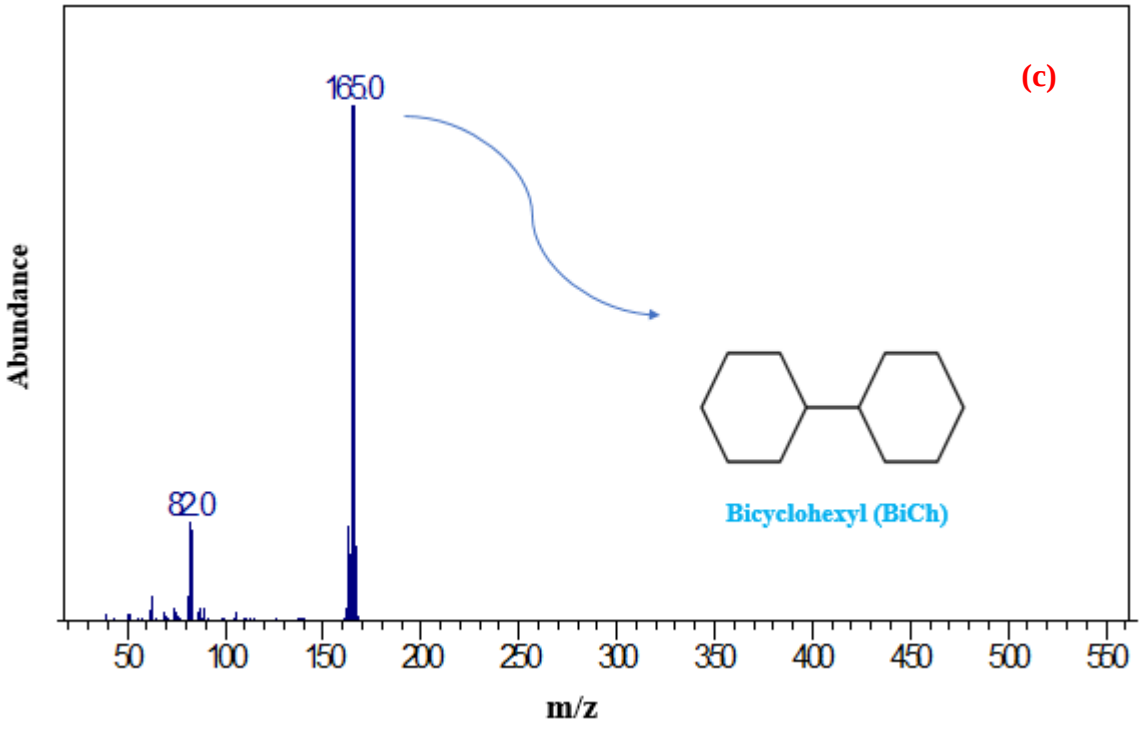

Figure 24 Gas Chromatogram of HDS of DBT over (a) AlCNFMoCo (b) Fragments of GC-SM corresponding to biphenyl product (c) and corresponding to the bicyclohexyl product.

5.4 Conclusion

The results of the hydrodesulfurization (HDS) reactions demonstrated that doping alumina with carbon nanofiber could enhance the degradation of the dibenzothiophene using an AlCNFMoCo catalyst. The results obtained using BET analysis of the AlCNFMoCo indicated that introducing CNF as a co-support enhanced the surface and textural properties of the MoCo catalysts, including the surface area, pore size, and the HF factor, which were contributing factors that improved catalytic efficiency. The HDS reaction was proposed with two main pathway reactions, namely, the hydrogenolysis pathway (DDS) and the hydrogenation desulfurization (HYD) pathway. Based on the GC-SM analysis, the HDS reaction pathway over the AlCNFMoCo catalyst can be considered to be a DDS reaction mechanism. Overall, the AlCNFMoCo catalyst could reduce the sulfur level down below

the allowed level, thus, the reported catalyst could be promising for use in industrial applications.

References

[1] I. Ahmed, S.H. Jhung, Adsorptive desulfurization and denitrogenation using metal-organic frameworks, J. Hazard. Mater. 301 (2016) 259–276. doi:10.1016/j.jhazmat.2015.08.045.

[2] R.S.C. Advances, V.C. Srivastava, RSC Advances An evaluation of desulfurization technologies for sulfur removal from liquid fuels, RSC Adv. (2012) 759–783. doi:10.1039/c1ra00309g.

[3] S.P. Hernandez, D. Fino, N. Russo, High performance sorbents for diesel oil desulfurization, Chem. Eng. Sci. 65 (2010) 603–609. doi:10.1016/j.ces.2009.06.050.

[4] M.H. Ibrahim, M.A. Hashim, A. Hayyan, The role of ionic liquids in desulfurization of fuels : A review, Renew. Sustain. Energy Rev. 76 (2017) 1534–1549. doi:10.1016/j.rser.2016.11.194.

[5] B.S. Huang, W.F. Yin, D.H. Sang, Z.Y. Jiang, Applied Surface Science Synergy effect of naphthenic acid corrosion and sulfur corrosion in crude oil distillation unit, Appl. Surf. Sci. 259 (2012) 664–670. doi:10.1016/j.apsusc.2012.07.094.

[6] P.P. Alvisi, V.F.C. Lins, An overview of naphthenic acid corrosion in a vacuum distillation plant, Eng. Fail. Anal. 18 (2011) 1403–1406. doi:10.1016/j.engfailanal.2011.03.019.

[7] J.H. Kim, X. Ma, A. Zhou, C. Song, Ultra-deep desulfurization and denitrogenation of diesel fuel by selective adsorption over three different adsorbents : A study on adsorptive selectivity and mechanism, Catal. Today. 111 (2006) 74–83. doi:10.1016/j.cattod.2005.10.017.

[8] Q. Wan, S.J. Danishefsky, Free-Radical-Based , Specific Desulfurization of Cysteine : A Powerful Advance in the Synthesis of Polypeptides and Glycopolypeptides, Angw. Chem.Int. 46 (2007) 9248–9252. doi:10.1002/anie.200704195.

[9] C. Song, X. Ma, New design approaches to ultra-clean diesel fuels by deep desulfurization and deep dearomatization, Appl. Catal. B Environ. 41 (2003) 207–238.

[10] X. Ma, L. Sun, C. Song, A new approach to deep desulfurization of gasoline ,

diesel fuel and jet fuel by selective adsorption for ultra-clean fuels and for fuel cell applications, Catal. Today. 77 (2002) 107–116.

[11] A. Stanislaus, A. Marafi, M.S. Rana, Recent advances in the science and technology of ultra low sulfur diesel (ULSD) production, Catal. Today. 153 (2010) 1–68. doi:10.1016/j.cattod.2010.05.011.

[12] C. Bouchy, F. Diehl, S. Brunet, D. Mey, G. Pe, On the hydrodesulfurization of FCC gasoline : a review, Appl. Catal. A. 278 (2005) 143–172. doi:10.1016/j.apcata.2004.10.012.

[13] F. Bataille, J.L. Lemberton, G. Pérot, P. Leyrit, T. Cseri, N. Marchal, S. Kasztelan, Sulfided Mo and CoMo supported on zeolite as hydrodesulfurization catalysts: Transformation of dibenzothiophene and 4,6-dimethyldibenzothiophene, Appl. Catal. A Gen. 220 (2001) 191–205. doi:10.1016/S0926-860X(01)00721-9.

[14] S. Damyanova, L. Petrov, M.A. Centeno, P. Grange, Characterization of molybdenum hydrodesulfurization catalysts supported on ZrO_2 -Al_2O_3 and ZrO_2 - SiO_2 carriers, Appl. Catal. A Gen. 224 (2002) 271–284.

[15] H. Farag, I. Mochida, K. Sakanishi, Fundamental comparison studies on hydrodesulfurization of dibenzothiophenes over CoMo-based carbon and alumina catalysts, Appl. Catal. A Gen. 195 (2000) 147–157.

[16] L. Datsevich, A. Jess, A. Lauter, C. Schmitz, P. Wasserscheid, Deep desulfurization of diesel fuel by extraction with ionic liquids, Chem. Commun. (2005) 2–3. doi:10.1039/b108411a.

[17] C. Huang, B. Chen, J. Zhang, Z. Liu, Y. Li, Desulfurization of Gasoline by Extraction with New Ionic Liquids, Energy & Fuels. (2004) 1862–1864. doi:10.1021/ef049879k.

[18] Y. Wang, R.T. Yang, Desulfurization of Liquid Fuels by Adsorption on Carbon-Based Sorbents and Ultrasound-Assisted Sorbent Regeneration, Langmuir. (2007) 3825–3831. doi:10.1021/la063364z.

[19] T.A. Saleh, S.A. Al-Hammadi, A. Tanimu, K. Alhooshani, Ultra-deep adsorptive desulfurization of fuels on cobalt and molybdenum nanoparticles loaded on activated carbon derived from waste rubber, J. Colloid Interface Sci. 513 (2018) 779–787. doi:10.1016/j.jcis.2017.11.076.

[20] H. Mei, B.W. Mei, T.F. Yen, A new method for obtaining ultra-low sulfur diesel fuel via ultrasound assisted oxidative desulfurization, Fuel. 82 (2003) 405–414. doi:10.1016/S0016-2361(02)00318-6.

[21] G. Yu, S. Lu, H. Chen, Z. Zhu, Oxidative Desulfurization of Diesel Fuels with Hydrogen Peroxide in the Presence of Activated Carbon and Formic Acid, Energy & Fuels. (2005) 447–452. doi:10.1021/ef049760b.

[22] K.O.H.T.A.R.O. Kirimura, T. Furuya, Y. Nishii, Y. Ishii, K. Kino, S. Usami,

Biodesulfurization of Dibenzothiophene and Its Derivatives through the Selective Cleavage of Carbon-Sulfur Bonds by a Moderately Thermophilic Bacterium Bacillus subtilis WU-S2B, J. Biosci. Bioeng. 91 (2001) 262–266.

[23] D.S. Reichmuth, J.L. Hittle, H.W. Blanch, J.D. Keasling, Biodesulfurization of Dibenzothiophene in Escherichia coli Is Enhanced by Expression of a Vibrio harveyi Oxidoreductase Gene, Biotechnol. Bioeng. 67 (2000).

[24] F. Davoodi-dehaghani, M. Vosoughi, A. Ali, Bioresource Technology Biodesulfurization of dibenzothiophene by a newly isolated Rhodococcus e rythropolis strain, Bioresour. Technol. 101 (2010) 1102–1105. doi:10.1016/j.biortech.2009.08.058.

[25] I. V Babich, J.A. Moulijn, Science and technology of novel processes for deep desulfurization of oil refinery streams : a review, Fuel. 82 (2003) 607–631.

[26] J. Ancheyta, M.S. Rana, V. Sa, J.A.I. Diaz, A review of recent advances on process technologies for upgrading of heavy oils and residua, Fuel. 86 (2007) 1216–1231. doi:10.1016/j.fuel.2006.08.004.

[27] L.C. Casta, J.A.D. Mu, J. Ancheyta, Current situation of emerging technologies for upgrading of heavy oils, Catal. Today. 222 (2014) 248–273. doi:10.1016/j.cattod.2013.05.016.

[28] S.K. Bej, S.K. Maity, U.T. Turaga, Catalyst : A Review of Recent Studies, Search an Effic. 4,6-DMDBT Hydrodesulfurization Catal. A Rev. Recent Stud. 18 (2005).

[29] E. Kianpour, S. Azizian, Polyethylene glycol as a green solvent for effective extractive desulfurization of liquid fuel at ambient conditions, FUEL. 137 (2014) 36–40. doi:10.1016/j.fuel.2014.07.096.

[30] Y. Nie, C. Li, A. Sun, H. Meng, Z. Wang, Extractive Desulfurization of Gasoline Using Imidazolium-Based Phosphoric Ionic Liquids, Energy & Fuels. (2006) 2083–2087. doi:10.1021/ef060170i.

[31] N.H. Ko, J.S. Lee, E.S. Huh, H. Lee, K.D. Jung, H.S. Kim, M. Cheong, Extractive Desulfurization Using Fe-Containing Ionic Liquids, Energy & Fuels. (2008) 1687–1690.

[32] Y. Zhang, Y. Yang, H. Han, M. Yang, L. Wang, Y. Zhang, Z. Jiang, C. Li, Environmental Ultra-deep desulfurization via reactive adsorption on Ni / ZnO : The effect of ZnO particle size on the adsorption performance, "Applied Catal. B, Environ. 119–120 (2012) 13–19. doi:10.1016/j.apcatb.2012.02.004.

[33] J.G. Park, C.H. Ko, K.B. Yi, J. Park, S. Han, S. Cho, J. Kim, Reactive adsorption of sulfur compounds in diesel on nickel supported on mesoporous silica, Appl. Catal. B Environ. 81 (2008) 244–250. doi:10.1016/j.apcatb.2007.12.014.

[34] X. Ma, S. Velu, J.H. Kim, C. Song, Deep desulfurization of gasoline by selective adsorption over solid adsorbents and impact of analytical methods on ppm-level

sulfur quantification for fuel cell applications, Appl. Catal. B Environ. 56 (2005) 137–147. doi:10.1016/j.apcatb.2004.08.013.

[35] D. Jayne, Y. Zhang, S. Haji, C. Erkey, Dynamics of removal of organosulfur compounds from diesel by adsorption on carbon aerogels for fuel cell applications , Hydrog. Energy. 30 (2005) 1287–1293. doi:10.1016/j.ijhydene.2005.03.014.

[36] J. Qiu, G. Wang, D. Zeng, Y. Tang, M. Wang, Y. Li, Oxidative desulfurization of diesel fuel using amphiphilic quaternary ammonium phosphomolybdate catalysts, Fuel Process. Technol. 90 (2009) 1538–1542. doi:10.1016/j.fuproc.2009.08.001.

[37] H. Lü, J. Gao, Z. Jiang, F. Jing, Y. Yang, G. Wang, C. Li, Ultra-deep desulfurization of diesel by selective oxidation with [$C_{18}H_{37}N(CH_3)_3]_4$[H_2 NaPW 10 O 36] catalyst assembled in emulsion droplets, J. Catal. 239 (2006) 369–375. doi:10.1016/j.jcat.2006.01.025.

[38] M. Soleimani, A. Bassi, A. Margaritis, Biodesulfurization of refractory organic sulfur compounds in fossil fuels, Biotechnol. Adv. 25 (2007) 570–596. doi:10.1016/j.biotechadv.2007.07.003.

[39] G. Mohebali, A.S. Ball, International Biodeterioration & Biodegradation Biodesulfurization of diesel fuels e Past , present and future perspectives, Int. Biodeterior. Biodegradation. 110 (2016) 163–180. doi:10.1016/j.ibiod.2016.03.011.

[40] P. Schacht, G. Hernández, L. Cedeño, J.H. Mendoza, S. Ramírez, L. García, J. Ancheyta, Hydrodesulfurization activity of CoMo catalysts supported on stabilized TiO2, Energy and Fuels. 17 (2003) 81–86. doi:10.1021/ef020144u.

[41] E. Pedernera, R. Reimert, N.L. Nguyen, V. Van Buren, Deep desulfurization of middle distillates: Process adaptation to oil fractions' compositions, Catal. Today. 79–80 (2003) 371–381. doi:10.1016/S0920-5861(03)00066-X.

[42] L. Peña, D. Valencia, T. Klimova, CoMo/SBA-15 catalysts prepared with EDTA and citric acid and their performance in hydrodesulfurization of dibenzothiophene, Appl. Catal. B Environ. 147 (2014) 879–887. doi:10.1016/j.apcatb.2013.10.019.

[43] R. Hubaut, J. Altafulla, A. Rives, C. Scott, Characterization and HDS activities of mixed Fe – Mo sulphides supported on alumina and carbon, Fuel. 86 (2007) 743–749. doi:10.1016/j.fuel.2006.09.012.

[44] M.H. D. Yitzhaki, M. Landau, D. Berger, Deep desulfurization of heavy atmospheric gas oil with Co-Mo-A1 catalysts Effect of sulfur adsorption, Appl. Catal. A Gen. 122 (1995).

[45] F.T.T. Ng, I.K. Milad, Catalytic desulphurization of benzothiophene in an emulsion via in situ generated H_2, Appl. Catal. A. 200 (2000) 243–254.

[46] C. Lanju, G.U.O. Shaohui, Oxidative Desulfurization of Simulated Gasoline over Metal Oxide-loaded Molecular Sieve, Chin.J.Chem.Eng. 15 (2007) 520–523.

[47] F. Al-shahrani, T. Xiao, S.A. Llewellyn, S. Barri, Z. Jiang, H. Shi, G. Martinie, M.L.H. Green, Desulfurization of diesel via the H_2O_2 oxidation of aromatic sulfides to sulfones using a tungstate catalyst, Appl. Catal. B Environ. 73 (2007) 311–316. doi:10.1016/j.apcatb.2006.12.016.

[48] L. Yang, J. Li, X. Yuan, J. Shen, Y. Qi, One step non-hydrodesulfurization of fuel oil : Catalyzed oxidation adsorption desulfurization over HPWA-SBA-15, J. Mol. Catal. A Chem. 262 (2007) 114–118. doi:10.1016/j.molcata.2006.08.058.

[49] S. Liu, B. Wang, B. Cui, L. Sun, Deep desulfurization of diesel oil oxidized by Fe (VI) systems, Fuel. 87 (2008) 422–428. doi:10.1016/j.fuel.2007.05.029.

[50] W. Wang, S. Wang, H. Liu, Z. Wang, Desulfurization of gasoline by a new method of electrochemical catalytic oxidation, Fuel. 86 (2007) 2747–2753. doi:10.1016/j.fuel.2007.03.006.

[51] L. Garcı, G.A. Fuentes, M.E. Herna, F. Murrieta-guevara, F. Jime, Ultra-deep oxidative desulfurization of diesel fuel by the Mo / Al_2O_3 -H_2O_2 system : The effect of system parameters on catalytic activity, Appl. Catal. A Gen. 334 (2008) 366–373. doi:10.1016/j.apcata.2007.10.024.

[52] H. Gomez-bernal, A. Fraustro-cuevas, H.D. Guerra-gomez, R. Cuevas-garcia, Oxidative desulfurization of synthetic diesel using supported catalysts Part III . Support effect on vanadium-based catalysts, Catal. Today. 135 (2008) 244–254. doi:10.1016/j.cattod.2007.12.017.

[53] E. Deliyanni, M. Seredych, T.J. Bandosz, Interactions of 4 , 6-Dimethyldibenzothiophene with the Surface of Activated Carbons, Langmuir. 25 (2009) 9302–9312. doi:10.1021/la900854x.

[54] M. Angeles, J. Ram, G. Busca, A FT-IR study of the adsorption of indole , carbazole , over solid adsorbents and catalysts, Appl. Catal. A Gen. 224 (2002) 167–178.

[55] F. Richard, T. Boita, G. Pe, Reaction mechanism of 4 , 6-dimethyldibenzothiophene desulfurization over sulfided NiMoP / Al_2O_3 -zeolite catalysts, Appl. Catal. A Gen. 320 (2007) 69–79. doi:10.1016/j.apcata.2006.12.014.

[56] Y. Sano, K. Sugahara, K. Choi, Y. Korai, I. Mochida, Two-step adsorption process for deep desulfurization of diesel oil, Fuel. 84 (2005) 903–910. doi:10.1016/j.fuel.2004.11.019.

[57] K. Tang, L. Song, L. Duan, X. Li, J. Gui, Z. Sun, Deep desulfurization by selective adsorption on a heteroatoms zeolite prepared by secondary synthesis, Fuel Process. Technol. 9 (2007) 1–6. doi:10.1016/j.fuproc.2007.06.002.

[58] C. Ngamcharussrivichai, C. Chatratananon, S. Nuntang, Adsorptive removal of thiophene and benzothiophene over zeolites from Mae Moh coal fly ash, Fuel. 87

(2008) 2347–2351. doi:10.1016/j.fuel.2007.10.003.

[59] Y. Wang, R.T. Yang, J.M. Heinzel, Desulfurization of jet fuel by -complexation adsorption with metal halides supported on MCM-41 and SBA-15 mesoporous materials, Chem. Eng. J. 63 (2008) 356–365. doi:10.1016/j.ces.2007.09.002.

[60] T.A. Saleh, K.O. Sulaiman, S.A. AL-Hammadi, H. Dafalla, G.I. Danmaliki, Adsorptive desulfurization of thiophene, benzothiophene and dibenzothiophene over activated carbon manganese oxide nanocomposite: with column system evaluation, J. Clean. Prod. 154 (2017) 401–412. doi:10.1016/j.jclepro.2017.03.169.

[61] F. Li, Z. Zhang, J. Feng, X. Cai, P. Xu, Biodesulfurization of DBT in tetradecane and crude oil by a facultative thermophilic bacterium Mycobacterium goodii X7B, J. Biotechnol. 127 (2007) 222–228. doi:10.1016/j.jbiotec.2006.07.002.

[62] A. Caro, P. Leto, E. Garcı, Enhancement of dibenzothiophene biodesulfurization using b -cyclodextrins in oil-to-water media, Fuel. 86 (2007) 2632–2636. doi:10.1016/j.fuel.2007.02.033.

[63] M. Rashtchi, G.H. Mohebali, M.M. Akbarnejad, J. Towfighi, B. Rasekh, A. Keytash, Analysis of biodesulfurization of model oil system by the bacterium , strain RIPI-22, Biochem. Eng. J. 29 (2006) 169–173. doi:10.1016/j.bej.2005.08.034.

[64] I. Bagus, W. Gunam, Y. Yaku, M. Hirano, K. Yamamura, F. Tomita, T. Sone, K. Asano, Biodesulfurization of Alkylated Forms of Dibenzothiophene and Benzothiophene by Sphingomonas subarctica T7b, Soc. Biotechnol. 101 (2006) 322–327. doi:10.1263/jbb.101.322.

[65] W. Li, Y. Zhang, M.D. Wang, Y. Shi, Biodesulfurization of dibenzothiophene and other organic sulfur compounds by a newly isolated Microbacterium strain ZD-M2, FEMS Microbiol. Lett. 247 (2005) 45–50. doi:10.1016/j.femsle.2005.04.025.

[66] M. Ayala, R. Tinoco, V. Hernandez, Biocatalytic oxidation of fuel as an alternative to biodesulfurization, Fuel Process. Technol. (1998) 101–111.

[67] S. Marques, Dibenzothiophene desulfurization by Gordonia alkanivorans strain 1B using recycled paper sludge hydrolyzate, Chemosphere. 70 (2008) 967–973. doi:10.1016/j.chemosphere.2007.08.016.

[68] H.O. Shinobu Oda, Biodesulfurization of Dibenzothiophene with Rhodococcus erythropolis ATCC 53968 and Its Mutant in an Interface Bioreactor, J. Biofertilizers Biopestic. 94 (2002) 474–477.

[69] S. Guobin, Z. Huaiying, X. Jianmin, C. Guo, L. Wangliang, L. Huizhou, Biodesulfurization of hydrodesulfurized diesel oil with Pseudomonas delafieldii R-8 from high density culture, Biochem. Eng. J. 27 (2006) 305–309. doi:10.1016/j.bej.2005.07.003.

[70] M. Egorova, R. Prins, The role of Ni and Co promoters in the simultaneous HDS

of dibenzothiophene and HDN of amines over Mo / γ -Al_2O_3 catalysts, J. Catal. 241 (2006) 162–172. doi:10.1016/j.jcat.2006.04.011.

[71] J. Van Gestel, C. Dujardin, F. Maug, J.C. Duchet, Direct Aromatic C – N Bond Cleavage Evidenced in the Hydrodenitrogenation of 2 , 6-Dimethylaniline over Cobalt-Promoted Mo / Al_2O_3 Sulfide Catalysts : A Reactivity and FT-IR Study, J. Catal. 88 (2001) 78–88. doi:10.1006/jcat.2001.3271.

[72] D. Liu, A. Wang, C. Liu, R. Prins, Ni 2 P / Al 2 O 3 hydrodesulfurization catalysts prepared by separating the nickel compound and hypophosphite, Catal. Today. 292 (2017) 133–142. doi:10.1016/j.cattod.2016.09.019.

[73] S.T. Oyama, T. Gott, H. Zhao, Y. Lee, Transition metal phosphide hydroprocessing catalysts : A review, Catal. Today. 143 (2009) 94–107. doi:10.1016/j.cattod.2008.09.019.

[74] R. Navarro, Deep hydrodesulfurization of DBT and diesel fuel on supported Pt and Ir catalysts, Appl. Catal. A Gen. 137 (1996) 269–286.

[75] A.M. Venezia, V. La Parola, G. Deganello, B. Pawelec, J.L.G. Fierro, Synergetic effect of gold in Au/Pd catalysts during hydrodesulfurization reactions of model compounds, J. Catal. 215 (2003) 317–325. doi:10.1016/S0021-9517(03)00005-8.

[76] Y. Okamoto, S. Ishihara, M. Kawano, M. Satoh, T. Kubota, Preparation of Co – Mo / Al 2 O 3 model sulfide catalysts for hydrodesulfurization and their application to the study of the effects of catalyst preparation, J. Catal. 217 (2003) 12–22. doi:10.1016/S0021-9517(03)00029-0.

[77] J. Ramirez, L. Cedeño, G. Busca, The role of titania support in Mo-based hydrodesulfurization catalysts, J. Catal. 184 (1999) 59–67. doi:10.1006/jcat.1999.2451.

[78] D.C. Phillips, S.J. Sawhill, R. Self, M.E. Bussell, Synthesis, Characterization, and Hydrodesulfurization Properties of Silica-Supported Molybdenum Phosphide Catalysts, J. Catal. 207 (2002) 266–273. doi:10.1006/jcat.2002.3524.

[79] R. Cattaneo, T. Shido, R. Prins, The Relationship between the Structure of NiMo / SiO 2 Catalyst Precursors Prepared in the Presence of Chelating Ligands and the Hydrodesulfurization Activity of the Final Sulfided Catalysts, J. Catal. 212 (1999) 199–212.

[80] S. Badoga, R. V Sharma, A.K. Dalai, J. Adjaye, Hydrotreating of heavy gas oil on mesoporous zirconia supported NiMo catalyst with EDTA, FUEL. 128 (2014) 30–38. doi:10.1016/j.fuel.2014.02.056.

[81] S. Bendezú, R. Cid, J.L.G. Fierro, A.L. Agudo, Thiophene hydrodesulfurization on sulfided Ni , W and NiW / USY zeolite catalysts : effect of the preparation method, Appl. Catal. A Gen. 197 (2000) 47–60.

[82] J.J. Lee, S. Han, H. Kim, J.H. Koh, T. Hyeon, S.H. Moon, Performance of CoMoS

catalysts supported on nanoporous carbon in the hydrodesulfurization of dibenzothiophene and 4,6-dimethyldibenzothiophene, Catal. Today. 86 (2003) 141–149. doi:10.1016/S0920-5861(03)00408-5.

[83] B. Pawelec, R. Mariscal, J.L.G. Fierro, A. Greenwood, P.T. Vasudevan, Carbon-supported tungsten and nickel catalysts for hydrodesulfurization and hydrogenation reactions, Appl. Catal. A Gen. 206 (2001) 295–307.

[84] C. Pophal, F. Kameda, K. Hoshino, S. Yoshinaka, K. Segawa, Hydrodesulfurization of dibenzothiophene derivatives over TiO_2-$A1_2O_3$ supported sulfided molybdenum catalyst, Catal. Today. 39 (1997) 21–32.

[85] G. Murali Dhar, B.N. Srinivas, M.S. Rana, M. Kumar, S.K. Maity, Mixed oxide supported hydrodesulfurization catalysts - A review, Catal. Today. 86 (2003) 45–60. doi:10.1016/S0920-5861(03)00403-6.

[86] F. Liu, S. Xu, Y. Chi, D. Xue, A novel alumina-activated carbon composite supported NiMo catalyst for hydrodesulfurization of dibenzothiophene, Short Commun. 12 (2011) 521–524. doi:10.1016/j.catcom.2010.11.018.

[87] M.J. Vissenberg, Y. Van Der Meer, E.J.M. Hensen, V.H.J. De Beer, A.M. Van Der Kraan, R.A. Van Santen, J.A.R. Van Veen, The Effect of Support Interaction on the Sulfidability of Al 2 O 3 - and TiO 2 -Supported CoW and NiW Hydrodesulfurization Catalysts, Jouranal Catal. 163 (2001) 151–163. doi:10.1006/jcat.2000.3132.

[88] C. Geantet, P. Afanasiev, Recent studies on the preparation , activation and design of active phases and supports of hydrotreating catalysts, Catal. Today. 130 (2008) 3–13. doi:10.1016/j.cattod.2007.08.018.

[89] G. Pérot, Hydrotreating catalysts containing zeolites and related materials - Mechanistic aspects related to deep desulfurization, Catal. Today. 86 (2003) 111–128. doi:10.1016/S0920-5861(03)00407-3.

[90] M. Breysse, P. Afanasiev, C. Geantet, M. Vrinat, Overview of support effects in hydrotreating catalysts, Catal. Today. 86 (2003) 5–16. doi:10.1016/S0920-5861(03)00400-0.

[91] F. Dumeignil, K. Sato, M. Imamura, N. Matsubayashi, E. Payen, H. Shimada, Characterization and hydrodesulfurization activity of CoMo catalysts supported on boron-doped sol-gel alumina, Appl. Catal. A Gen. 315 (2006) 18–28. doi:10.1016/j.apcata.2006.08.034.

[92] D. Valencia, T. Klimova, I. García-Cruz, Aromaticity of five- and six-membered heterocycles present in crude oils - An electronic description for hydrotreatment process, Fuel. 100 (2012) 177–185. doi:10.1016/j.fuel.2012.05.011.

[93] R. Abro, A. a Abdeltawab, S.S. Al-deyab, G. Yu, A.B. Qazi, S. Gao, X. Chen, RSC Advances A review of extractive desulfurization of fuel oils, RSC Adv. 4

(2014) 35302–35317. doi:10.1039/C4RA03478C.

[94] A.J. Hernández-Maldonado, R.T. Yang, Desulfurization of Transportation Fuels by Adsorption, Catal. Rev. 46 (2004) 111–150. doi:10.1081/CR-200032697.

[95] E. Furimsky, Catalytic hydrodeoxygenation, Appl. Catal. A Gen. 199 (2000) 147–190.

[96] D.D. Whitehurst, T. Isoda, I. Mochida, Present State of the Art and Future Challenges in the Hydrodesulfurization of Polyaromatic Sulfur Compounds, Elsevier Masson SAS, 1998. doi:10.1016/S0360-0564(08)60631-8.

[97] G.G. Zeelani, A. Ashrafi, A. Dhakad, G. Gupta, S.L. Pal, A Review on Desulfurization Techniques of Liquid Fuels, Int. J. Sci. Res. 5 (2016) 331–336.

[98] E. Myszka, J.R. Grzechowiak, G. V. Smith, Influence of porous structure on HDS [hydrodesulfurization] activity of cobalt-molybdenum-nickel catalysts, Energy & Fuels. 3 (1989) 541–543. doi:10.1021/ef00017a001.

[99] L. Ding, Y. Zheng, Z. Zhang, Z. Ring, J. Chen, HDS, HDN, HDA, and hydrocracking of model compounds over Mo-Ni catalysts with various acidities, Appl. Catal. A Gen. 319 (2007) 25–37. doi:10.1016/j.apcata.2006.11.016.

[100] M.A. Domínguez-Crespo, A.M. Torres-Huerta, L. Díaz-García, E.M. Arce-Estrada, E. Ramírez-Meneses, HDS, HDN and HDA activities of nickel-molybdenum catalysts supported on alumina, Fuel Process. Technol. 89 (2008) 788–796. doi:10.1016/j.fuproc.2008.01.004.

[101] M. Hussain, S.-K. Ihm, Synthesis, Characterization, and Hydrodesulfurization Activity of New Mesoporous Carbon Supported Transition Metal Sulfide Catalysts, Ind. Eng. Chem. Res. 48 (2009) 698–707. doi:10.1021/ie801229y.

[102] Z. Yu, L.E. Fareid, K. Moljord, E.A. Blekkan, J.C. Walmsley, D. Chen, Hydrodesulfurization of thiophene on carbon nanofiber supported Co/Ni/Mo catalysts, Appl. Catal. B Environ. 84 (2008) 482–489. doi:10.1016/j.apcatb.2008.05.013.

[103] H. Yin, T. Zhou, Y. Liu, Y. Chai, C. Liu, NiMo/Al_2O_3 catalyst containing nano-sized zeolite y for deep hydrodesulfurization and hydrodenitrogenation of diesel, J. Nat. Gas Chem. 20 (2011) 441–448. doi:10.1016/S1003-9953(10)60204-6.

[104] Z. Zhao, H. Wu, A. Duan, T. Li, R. Prins, X. Zhou, Synthesis of NiMo hydrodesulfurization catalyst supported on a composite of nano-sized ZSM-5 zeolite enwrapped with mesoporous KIT-6 material and its high isomerization selectivity, J. Catal. 317 (2014) 303–317. doi:10.1016/j.jcat.2014.07.002.

[105] S.K. Maity, M.S. Rana, S.K. Bej, J. Ancheyta-Juárez, G. Murali Dhar, T.S.R. Prasada Rao, Studies on physico-chemical characterization and catalysis on high surface area titania supported molybdenum hydrotreating catalysts, Appl. Catal. A Gen. 205 (2001) 215–225. doi:10.1016/S0926-860X(00)00567-6.

[106] S. Inoue, A. Muto, H. Kudou, T. Ono, Preparation of novel titania support by applying the multi-gelation method for ultra-deep HDS of diesel oil, Appl. Catal. A Gen. 269 (2004) 7–12. doi:10.1016/j.apcata.2004.03.019.

[107] J. Ramírez, G. Macías, L. Cedeño, A. Gutiérrez-Alejandre, R. Cuevas, P. Castillo, The role of titania in supported Mo, CoMo, NiMo, and NiW hydrodesulfurization catalysts: Analysis of past and new evidences, Catal. Today. 98 (2004) 19–30. doi:10.1016/j.cattod.2004.07.050.

[108] K. CHARY, Structure and catalytic properties of molybdenum oxide catalysts supported on zirconia, J. Catal. 226 (2004) 283–291. doi:10.1016/j.jcat.2004.04.028.

[109] S.. Maity, M.. Rana, B.. Srinivas, S.. Bej, G. Murali Dhar, T.S. Prasada Rao, Characterization and evaluation of ZrO2 supported hydrotreating catalysts, J. Mol. Catal. A Chem. 153 (2000) 121–127. doi:10.1016/S1381-1169(99)00311-8.

[110] G.A. Fuentes, C. Salcedo, T. Klimova, O.Y. Gutie, SBA-15 supports modified by Ti and Zr grafting for NiMo hydrodesulfurization catalysts, Catal. Today. 116 (2006) 485–497. doi:10.1016/j.cattod.2006.06.035.

[111] M.Á. Calderón-Magdaleno, J.A. Mendoza-Nieto, T.E. Klimova, Effect of the amount of citric acid used in the preparation of NiMo/SBA-15 catalysts on their performance in HDS of dibenzothiophene-type compounds, Catal. Today. 220–222 (2014) 78–88. doi:10.1016/j.cattod.2013.06.002.

[112] F. Cui, G. Li, X. Li, M. Lu, M. Li, Enhancement of hydrodesulfurization of 4,6-dimethyldibenzothiophene catalyzed by CoMo catalysts supported on carbon-covered γ-Al 2 O 3, Catal. Sci. Technol. 5 (2015) 549–555. doi:10.1039/C4CY00814F.

[113] Q. Guan, X. Cheng, R. Li, W. Li, A feasible approach to the synthesis of nickel phosphide for hydrodesulfurization, J. Catal. 299 (2013) 1–9. doi:10.1016/j.jcat.2012.11.008.

[114] S. Bharech, R. Kumar, A Review on the Properties and Applications of Graphene, J. Mater. Sci. Mech. Eng. 2 (2015) 70–73.

[115] H. Nguyen Bich, H. Nguyen Van, Promising applications of graphene and graphene-based nanostructures, Adv. Nat. Sci. Nanosci. Nanotechnol. 7 (2016). doi:10.1088/2043-6262/7/2/023002.

[116] P. V. Kamat, Graphene-based nanoarchitectures. Anchoring semiconductor and metal nanoparticles on a two-dimensional carbon support, J. Phys. Chem. Lett. 1 (2010) 520–527. doi:10.1021/jz900265j.

[117] A. A Abdala, Applications of Graphene in Catalysis, J. Biofertilizers Biopestic. 5 (2014). doi:10.4172/2157-7544.1000132.

[118] X. Zhou, J. Qiao, L. Yang, J. Zhang, A review of graphene-based nanostructural

materials for both catalyst supports and metal-free catalysts in PEM fuel cell oxygen reduction reactions, Adv. Energy Mater. 4 (2014) 1–25. doi:10.1002/aenm.201301523.

[119] J. Ping, Y. Zhou, Y. Wu, V. Papper, S. Boujday, R.S. Marks, T.W.J. Steele, Recent advances in aptasensors based on graphene and graphene-like nanomaterials, Biosens. Bioelectron. 64 (2015) 373–385. doi:10.1016/j.bios.2014.08.090.

[120] M.D. Stoller, S. Park, Z. Yanwu, J. An, R.S. Ruoff, Y. Zhu, J. An, R.S. Ruoff, Z. Yanwu, J. An, R.S. Ruoff, Graphene-Based ultracapacitors, Nano Lett. 8 (2008) 3498–3502. doi:10.1021/nl802558y.

[121] M.A. Al-Daous, Graphene-MoS2composite: Hydrothermal synthesis and catalytic property in hydrodesulfurization of dibenzothiophene, Catal. Commun. 72 (2015) 180–184. doi:10.1016/j.catcom.2015.09.030.

[122] X. Wang, W. Xu, N. Liu, Z. Yu, Y. Li, J. Qiu, Synthesis of metallic Ni-Co/graphene catalysts with enhanced hydrodesulfurization activity via a low-temperature plasma approach, Catal. Today. 256 (2015) 203–208. doi:10.1016/j.cattod.2015.04.026.

[123] Z. Hajjar, M. Kazemeini, A. Rashidi, M. Bazmi, Graphene based catalysts for deep hydrodesulfurization of naphtha and diesel fuels: A physiochemical study, Fuel. 165 (2016) 468–476. doi:10.1016/j.fuel.2015.10.040.

[124] H. Wang, B. Xiao, X. Cheng, C. Wang, L. Zhao, Y. Zhu, J. Zhu, X. Lu, NiMo catalysts supported on graphene-modified mesoporous TiO_2 toward highly efficient hydrodesulfurization of dibenzothiophene, Appl. Catal. A Gen. 502 (2015) 157–165. doi:10.1016/j.apcata.2015.05.028.

[125] J. Peréz-Ramírez, D. Verboekend, A. Bonilla, S. Abelló, Zeolite catalysts with tunable hierarchy factor by pore-growth moderators, Adv. Funct. Mater. 19 (2009) 3972–3979. doi:10.1002/adfm.200901394.

[126] I. Eswaramoorthi, V. Sundaramurthy, N. Das, A.K. Dalai, J. Adjaye, Application of multi-walled carbon nanotubes as efficient support to NiMo hydrotreating catalyst, Appl. Catal. A Gen. 339 (2008) 187–195. doi:10.1016/j.apcata.2008.01.021.

[127] Y. Wang, Y. Li, L. Tang, J. Lu, J. Li, Application of graphene-modified electrode for selective detection of dopamine, Electrochem. Commun. 11 (2009) 889–892. doi:10.1016/j.elecom.2009.02.013.

[128] H. Wang, B. Xiao, X. Cheng, C. Wang, L. Zhao, Y. Zhu, J. Zhu, X. Lu, NiMo catalysts supported on graphene-modified mesoporous TiO_2 toward highly efficient hydrodesulfurization of dibenzothiophene, Appl. Catal. A Gen. 502 (2015) 157–165. doi:10.1016/j.apcata.2015.05.028.

[129] N.O. Tio, V. Santes, J. Herbert, T. Cortez, L. Dı, B. Medellı, Hydrotreating Activity of Heavy Gasoil over NiMo/γ-Al_2O_3–TiO_2, Pet. Sci. Technol. 22 (2004) 103–117. doi:10.1081/LFT-120028526.

[130] M.Á. Calderón-Magdaleno, J.A. Mendoza-Nieto, T.E. Klimova, Effect of the amount of citric acid used in the preparation of NiMo/SBA-15 catalysts on their performance in HDS of dibenzothiophene-type compounds, Catal. Today. 220–222 (2014) 78–88. doi:10.1016/j.cattod.2013.06.002.

[131] M. Lewandowski, Z. Sarbak, Effect of boron addition on hydrodesulfurization and hydrodenitrogenation activity of NiMo/Al2O3catalysts, Fuel. 79 (2000) 487–495. doi:10.1016/S0016-2361(99)00151-9.

[132] M.S. Solum, R.J. Pugmire, M. Jagtoyen, F. Derbyshire, Evolution of carbon structure in chemically activated wood, Carbon N. Y. 33 (1995) 1247–1254. doi:10.1016/0008-6223(95)00067-N.

[133] E. Fuente, J.A. Menéndez, M.A. Díez, D. Suárez, M.A. Montes-Morán, J.A. Menendez, M.A. Diez, D. Suarez, M.A. Montes-Moran, Infrared Spectroscopy of Carbon Materials: A Quantum Chemical Study of Model Compounds, J. Phys. Chem. B. 107 (2003) 6350–6359. doi:10.1021/jp027482g.

[134] D. Valencia, L. Peña, I. García-Cruz, Reaction mechanism of hydrogenation and direct desulfurization routes of dibenzothiophene-like compounds: A density functional theory study, Int. J. Quantum Chem. 112 (2012) 3599–3605. doi:10.1002/qua.24242.

[135] O. V. Klimov, A. V. Pashigreva, M.A. Fedotov, D.I. Kochubey, Y.A. Chesalov, G.A. Bukhtiyarova, A.S. Noskov, Co-Mo catalysts for ultra-deep HDS of diesel fuels prepared via synthesis of bimetallic surface compounds, J. Mol. Catal. A Chem. 322 (2010) 80–89. doi:10.1016/j.molcata.2010.02.020.

[136] S. Eijsbouts, A.A. Battiston, G.C. Van Leerdam, Life cycle of hydroprocessing catalysts and total catalyst management, 130 (2008) 361–373. doi:10.1016/j.cattod.2007.10.112.

[137] S.L. Amaya, G. Alonso-Núñez, T.A. Zepeda, S. Fuentes, A. Echavarría, Effect of the divalent metal and the activation temperature of NiMoW and CoMoW on the dibenzothiophene hydrodesulfurization reaction, Appl. Catal. B Environ. 148–149 (2014) 221–230. doi:10.1016/j.apcatb.2013.10.057.

[138] H.F. Mohd Zaid, F.K. Chong, M.I. Abdul Mutalib, Extractive deep desulfurization of diesel using choline chloride-glycerol eutectic-based ionic liquid as a green solvent, Fuel. 192 (2017) 10–17. doi:10.1016/j.fuel.2016.11.112.

[139] F.R. Moghadam, S. Azizian, M. Bayat, M. Yarie, E. Kianpour, M.A. Zolfigol, Extractive desulfurization of liquid fuel by using a green, neutral and task specific phosphonium ionic liquid with glyceryl moiety: A joint experimental and computational study, Fuel. 208 (2017) 214–222. doi:10.1016/j.fuel.2017.07.025.

[140] T.A. Saleh, G.I. Danmaliki, Adsorptive desulfurization of dibenzothiophene from fuels by rubber tyres-derived carbons : Kinetics and isotherms evaluation, Process Saf. Environ. Prot. 102 (2016) 9–19. doi:10.1016/j.psep.2016.02.005.

[141] B.K. Jung, S.H. Jhung, Adsorptive removal of benzothiophene from model fuel, using modified activated carbons, in presence of diethylether, Fuel. 145 (2015) 249–255. doi:10.1016/j.fuel.2014.12.088.

[142] G.I. Danmaliki, T.A. Saleh, Effects of bimetallic Ce/Fe nanoparticles on the desulfurization of thiophenes using activated carbon, Chem. Eng. J. 307 (2017) 914–927. doi:10.1016/j.cej.2016.08.143.

[143] S.K. Thaligari, V.C. Srivastava, B. Prasad, Adsorptive desulfurization by zinc-impregnated activated carbon: characterization, kinetics, isotherms, and thermodynamic modeling, Clean Technol. Environ. Policy. 18 (2016) 1021–1030. doi:10.1007/s10098-015-1090-y.

[144] S. Wei, H. He, Y. Cheng, C. Yang, G. Zeng, L. Kang, H. Qian, C. Zhu, Preparation, characterization, and catalytic performances of cobalt catalysts supported on KIT-6 silicas in oxidative desulfurization of dibenzothiophene, Fuel. 200 (2017) 11–21. doi:10.1016/j.fuel.2017.03.052.

[145] S. Otsuki, T. Nonaka, N. Takashima, W. Qian, A. Ishihara, T. Imai, T. Kabe, Oxidative Desulfurization of Light Gas Oil and Vacuum Gas Oil by Oxidation and Solvent Extraction, Energy & Fuels. 14 (2000) 1232–1239. doi:10.1021/ef000096i.

[146] D. Montalván-Sorrosa, D. De Los Cobos-Vasconcelos, A. González-Sánchez, Nanotechnology Applied to the Biodesulfurization of Fossil Fuels and Spent Caustic Streams, Appl. Nanotechnol. to Desulfurization Process Pet. Eng. (2016) 378–389. doi:10.4018/978-1-4666-9545-0.

[147] I. Martínez, V.E. Santos, F. Garcìa-Ochoa, Metabolic kinetic model for dibenzothiophene desulfurization through 4S pathway using intracellular compound concentrations, Biochem. Eng. J. 117 (2017) 89–96. doi:10.1016/j.bej.2016.11.004.

[148] I. Martínez, M. El-Said Mohamed, V.E. Santos, J.L. García, F. García-Ochoa, E. Díaz, Metabolic and process engineering for biodesulfurization in Gram-negative bacteria, J. Biotechnol. 262 (2017) 47–55. doi:10.1016/j.jbiotec.2017.09.004.

[149] A. V. Pashigreva, G.A. Bukhtiyarova, O. V. Klimov, Y.A. Chesalov, G.S. Litvak, A.S. Noskov, Activity and sulfidation behavior of the CoMo/Al2O3 hydrotreating catalyst: The effect of drying conditions, Catal. Today. 149 (2010) 19–27. doi:10.1016/j.cattod.2009.07.096.

[150] Y. Shu, S.T. Oyama, Synthesis, characterization, and hydrotreating activity of carbon-supported transition metal phosphides, Carbon N. Y. 43 (2005) 1517–1532. doi:10.1016/j.carbon.2005.01.036.

[151] G. Kishan, L. Coulier, V.H.J. de Beer, J.A.R. van Veen, J.W. Niemantsverdriet, Sulfidation and Thiophene Hydrodesulfurization Activity of Nickel Tungsten Sulfide Model Catalysts, Prepared without and with Chelating Agents, J. Catal. 196 (2000) 180–189. doi:10.1006/jcat.2000.3013.

[152] H. Purón, J.L. Pinilla, I. Suelves, M. Millan, Acid treated carbon nanofibers as catalytic support for heavy oil hydroprocessing, Catal. Today. 249 (2015) 79–85. doi:10.1016/j.cattod.2014.09.021.

[153] J.L. Pinilla, H. Purón, D. Torres, I. Suelves, M. Millan, Ni-MoS_2 supported on carbon nanofibers as hydrogenation catalysts: Effect of support functionalisation, Carbon N. Y. 81 (2015) 574–586. doi:10.1016/j.carbon.2014.09.092.

[154] D.A. Solís-Casados, A.L. Agudo, J. Ramírez, T. Klimova, Hydrodesulfurization of hindered dibenzothiophenes on bifunctional NiMo catalysts supported on zeolite-alumina composites, Catal. Today. 116 (2006) 469–477. doi:10.1016/j.cattod.2006.06.029.

[155] A. Barth, The infrared absorption of amino acid side chains, Prog. Biophys. Mol. Biol. 74 (2000) 141–173. doi:10.1016/S0079-6107(00)00021-3.

[156] Dong Jin Suh, P. Tae-Jin, I. Son-Ki, Effect of surface oxygen groups of carbon supports on the characteristics of Pd/C catalysts, Carbon N. Y. 31 (1993) 427–435. doi:10.1016/0008-6223(93)90130-3.

[157] H. Shang, C. Liu, Y. Xu, J. Qiu, F. Wei, States of carbon nanotube supported Mo-based HDS catalysts, Fuel Process. Technol. 88 (2007) 117–123. doi:10.1016/j.fuproc.2004.08.010.

Vitae

Name :SADDAM AHMED GHALEB AL-HAMMADI

Nationality :Yemen

Date of Birth :11/29/1990

Email :sadam80780@gmail.com

Address :Yemen, Sana'a

Academic Background :

Master of Science in Chemical Engineering, (Jan,2016-April 2018)

Bachelor of Science in Chemical Engineering, (Jan,2011-Jan 2016).

Publications

- S.A. AL-Hammadi, A.M. Al-Amer, T.A. Saleh, Alumina-carbon nanofiber composite as a support for MoCo catalysts in hydrodesulfurization reactions, Chemical Engineering Journal (2018).

- T.A. Saleh, S.A. AL-Hammadi, A. Tanimu, K. Alhooshani, Ultra-deep adsorptive desulfurization of fuels on cobalt and molybdenum nanoparticles loaded on activated carbon derived from waste rubber, Journal of Colloid and Interface Science (2017).

- T.A. Saleh, K.O. Sulaiman, S.A. Al-Hammadi, H. Dafalla, G.I. Danmaliki, Adsorptive desulfurization of thiophene, benzothiophene and dibenzothiophene over activated carbon manganese oxide nanocomposite: with column system evaluation, J. Clean. Prod. 154 (2017) 401–412.